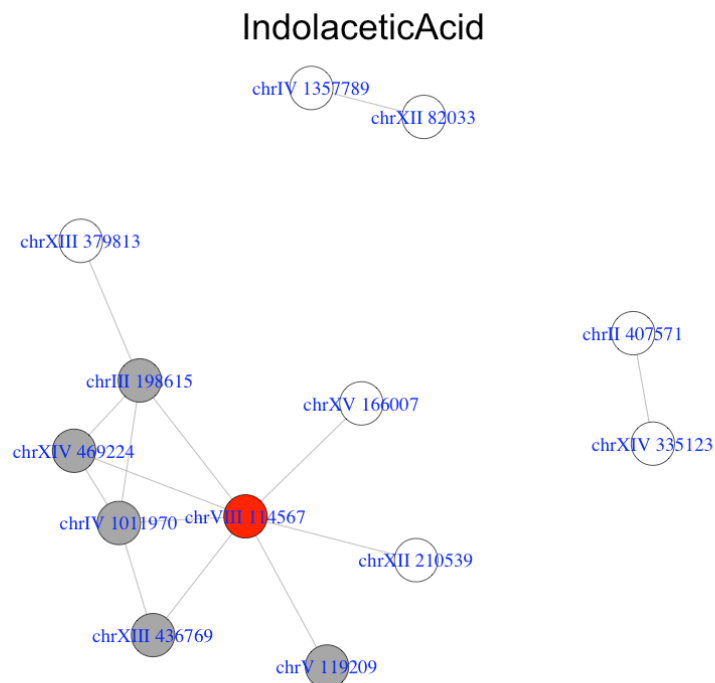
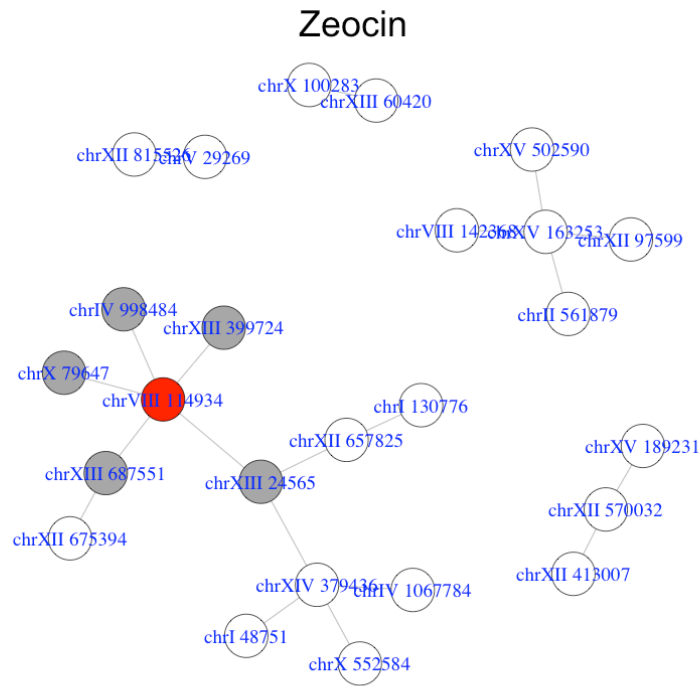


**Figure S1.** Histogram of the number of genetic interactions per locus. The X-axis gives the number of genetic interactions per locus and the Y-axis gives the number of loci. Most loci are only involved in one interaction and a few hub loci are involved in many.



**Figure S2.** Network of interacting loci detected for Indole Acetic Acid. Each circle represents one locus and connections represents pairwise genetic interactions. The position of

*the most significant SNP at each locus is given by the blue texts. The subset of the network analyzed in greater detail, with respect to phenotypic prediction and the effect of these interactions on the additive genetic variance, is colored in red and grey: The hub locus is colored in red and the 5 radial loci in grey. Results are represented in the same manner in figures S3-S12.*



**Figure S3. Network of interacting loci detected for Zeocin.**

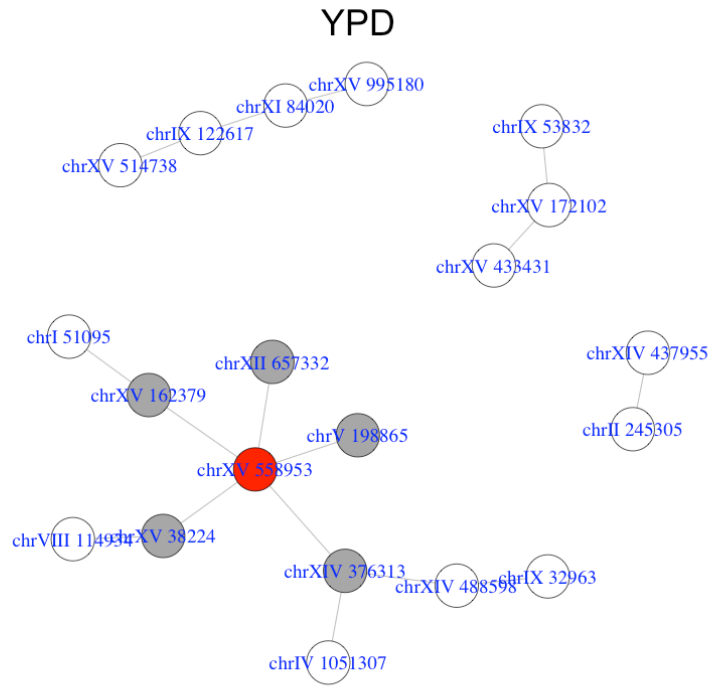


**Figure S4. Network of interacting loci detected for YPD.**

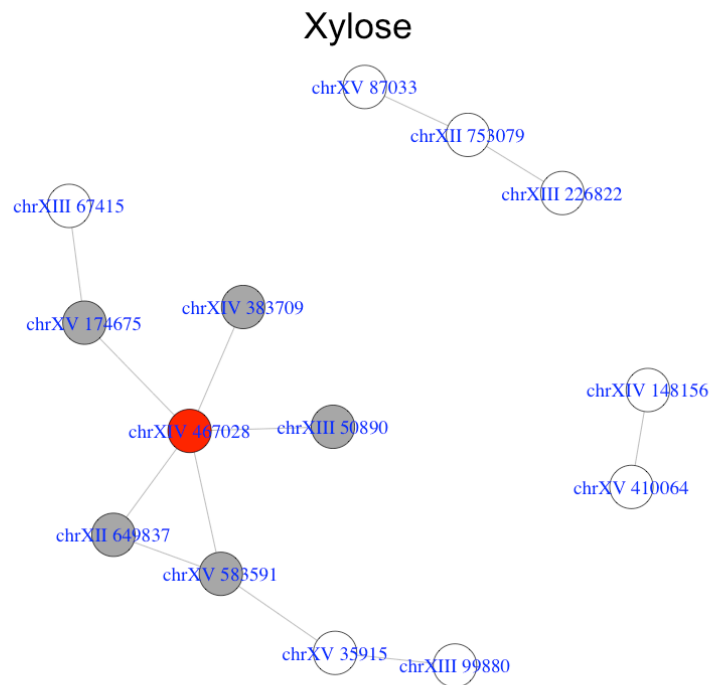


**Figure S5. Network of interacting loci detected for Xylose.**

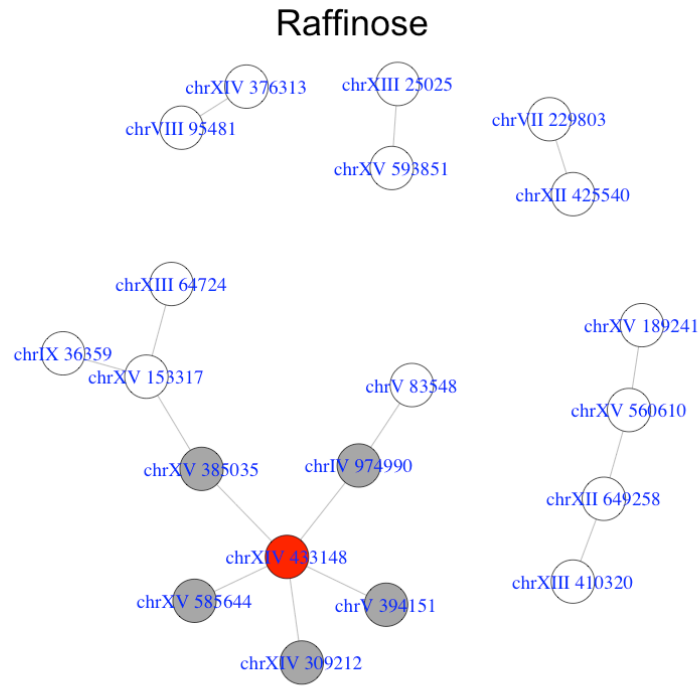


**Figure S6. Network of interacting loci detected for Raffinose.**

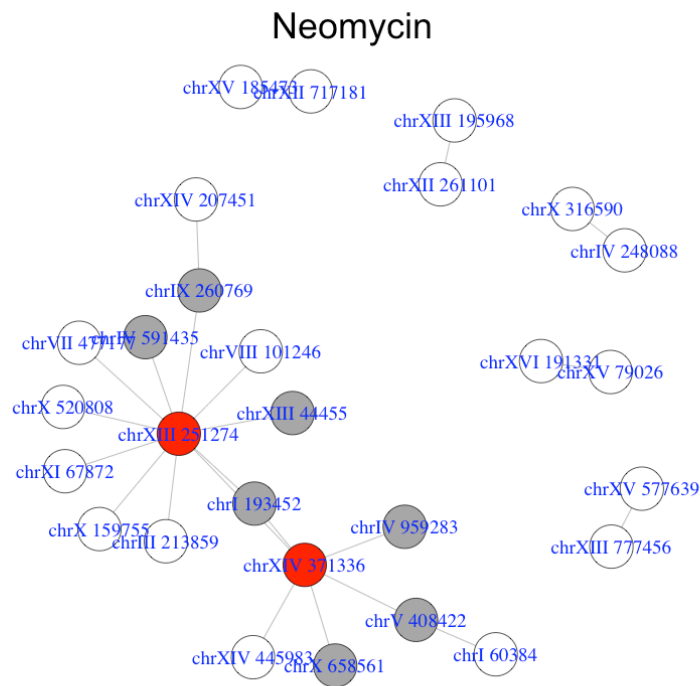


**Figure S7. Network of interacting loci detected for Neomycin.**

## ManganeseSulfate

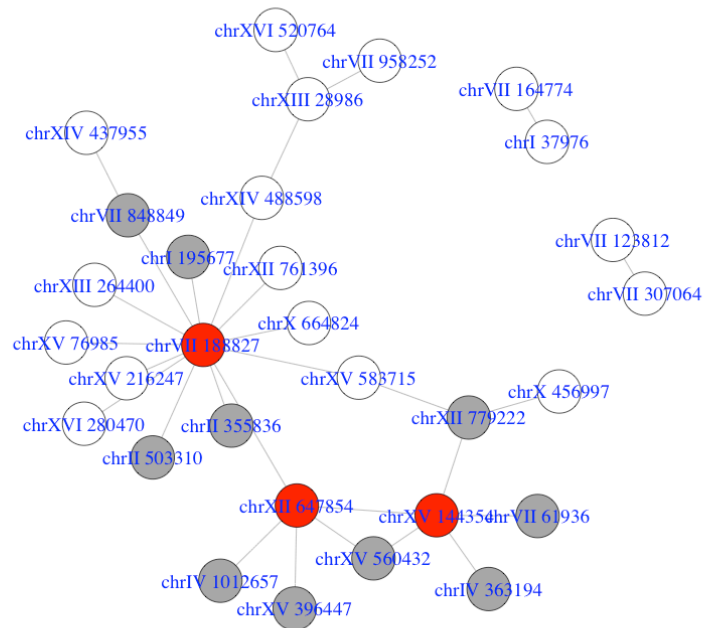


**Figure S8.** Network of interacting loci detected for Manganese Sulfate.

## Lactate

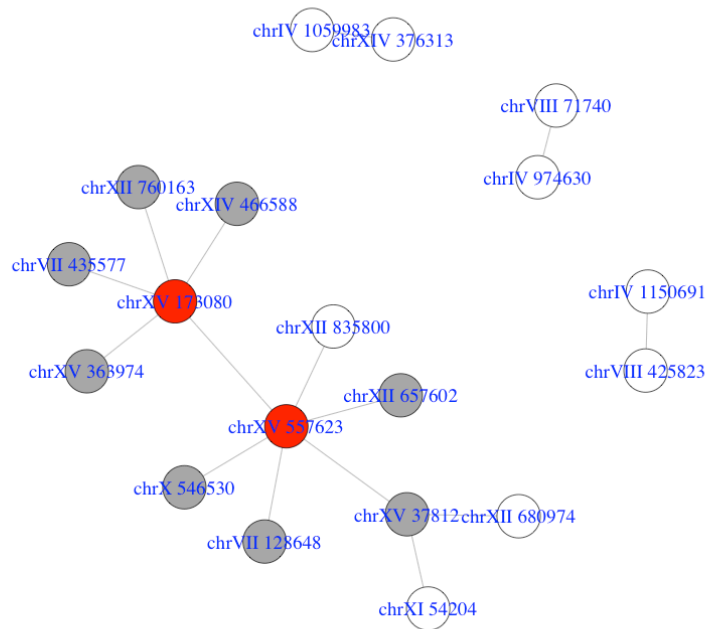


**Figure S9.** Network of interacting loci detected for Lactate.

### E6-Berberamine

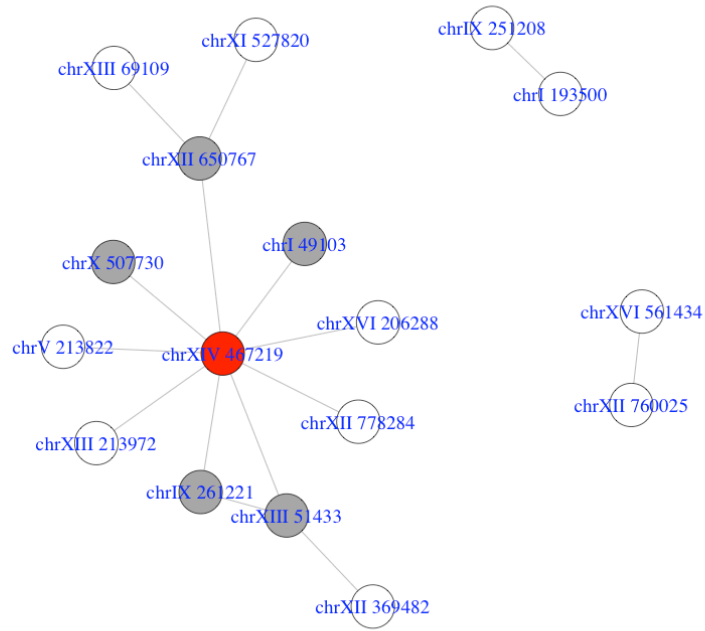


**Figure S10.** Network of interacting loci detected for E6-Berberamine.

### CopperSulfate

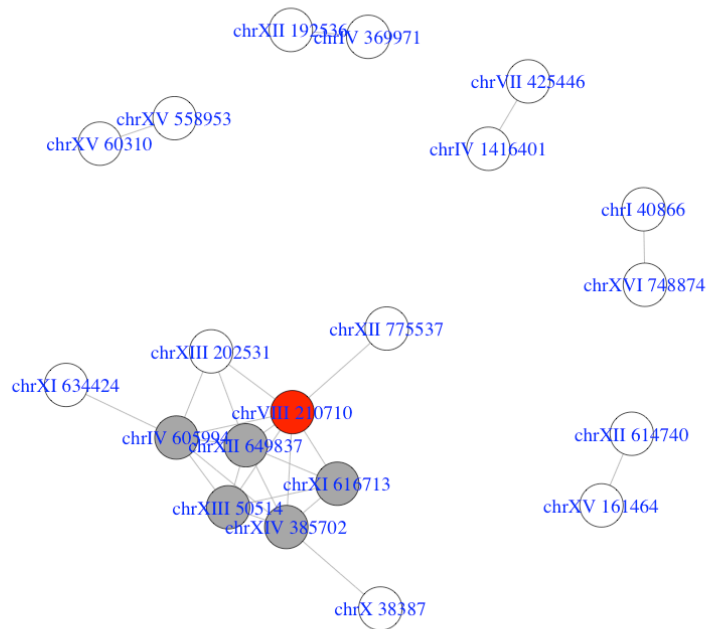


**Figure S11.** Network of interacting loci detected for Copper Sulfate.

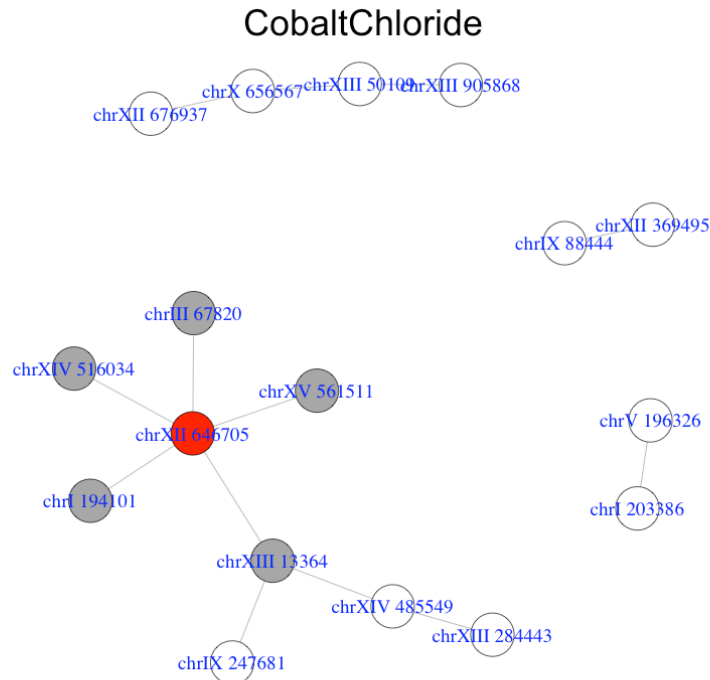


**Figure S12. Network of interacting loci detected for Cobalt Chloride.**

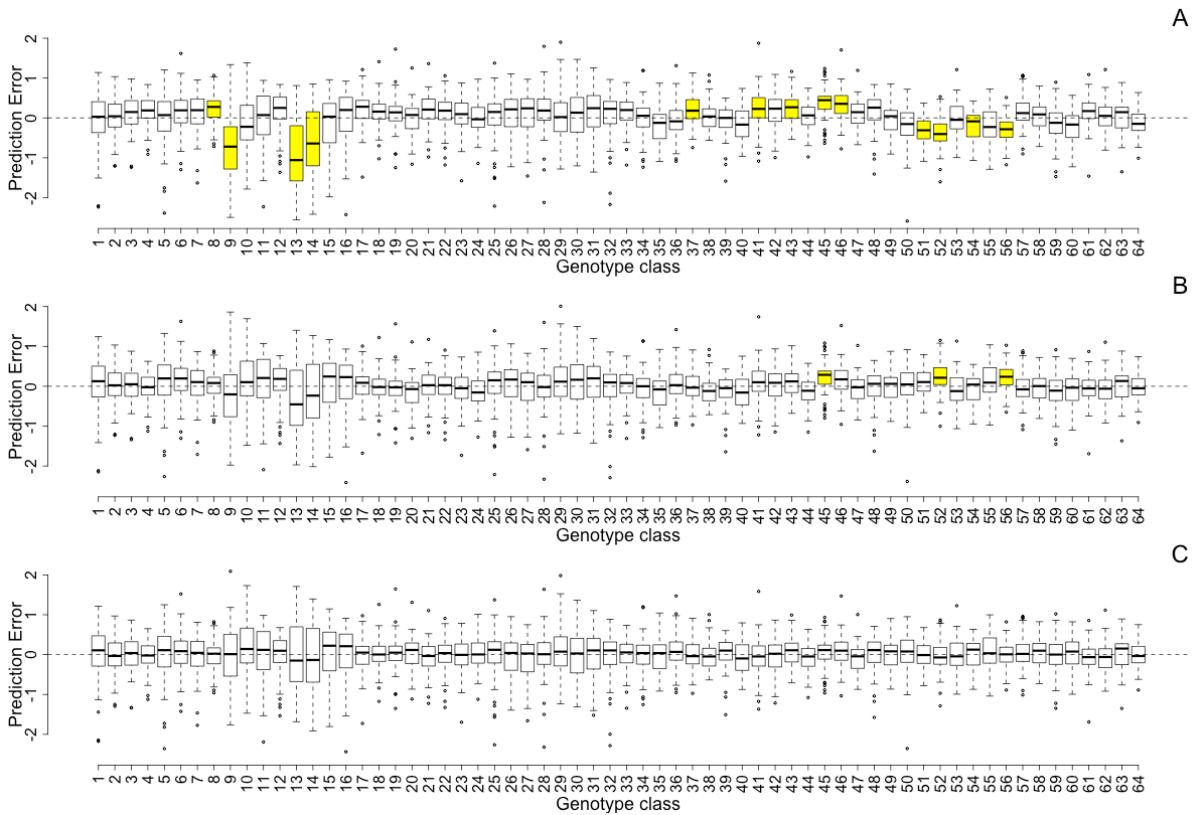


**Figure S13. Phenotypic prediction accuracy Indole Acetic Acid.** The Y-axes show the prediction errors (residuals)  $y - y_{pred}$  from models including the 6 loci in the epistatic network regulating growth on Indole Acetic Acid (red and grey circles in figS2).  $y_{pred}$  is estimated using a 10-fold cross validation. The prediction errors are divided according to

which genotype class the predicted yeast segregant belongs to. Each boxplot thus shows the distribution of prediction errors in one genotype class. The genotype classes where the predictions are significantly biased, i.e. the prediction errors deviate significantly from zero, are colored in yellow. **A.** The prediction errors from a linear model including only additive effects. **B.** The prediction errors from a linear model including additive effects and selected pairwise genetic interactions. **C.** The prediction errors from a linear model including additive effects and selected pairwise, and three-way, genetic interactions. Results are represented in the same manner in figures S14-S26.

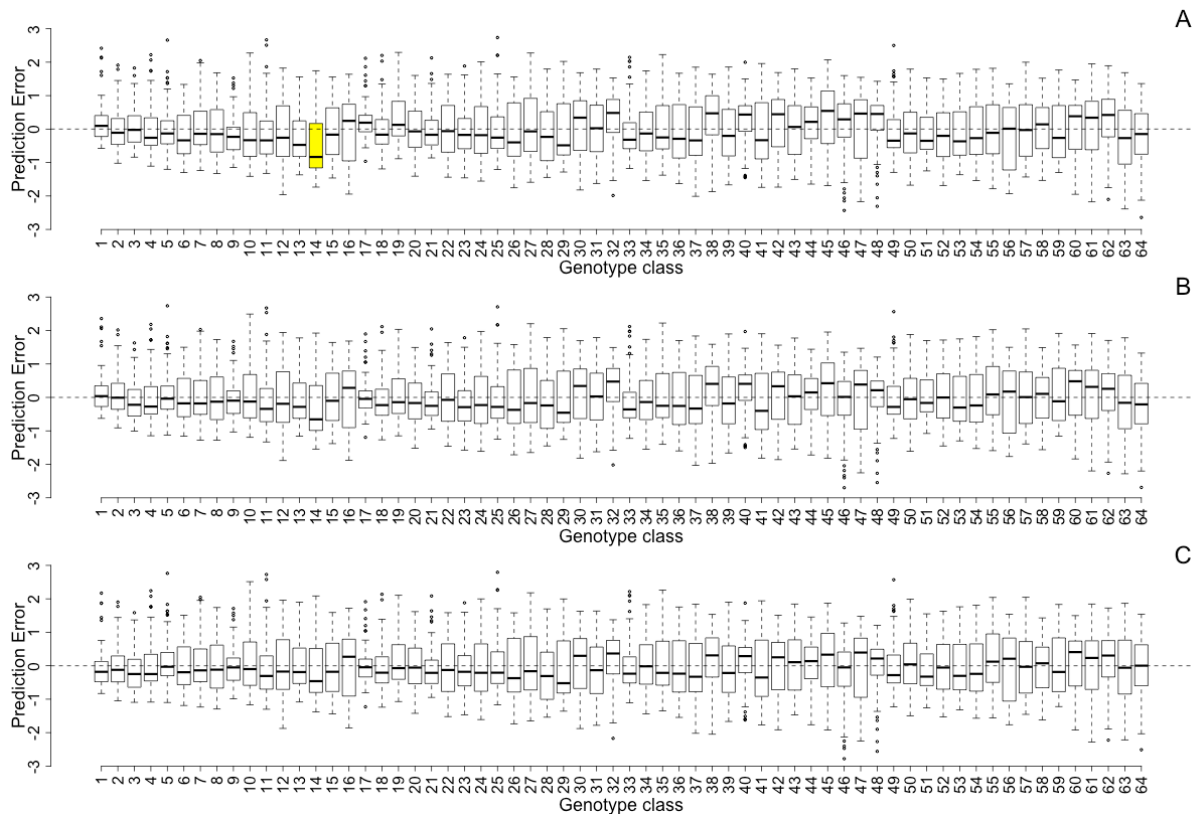


**Figure S14. Phenotypic prediction accuracy Zeocin.**



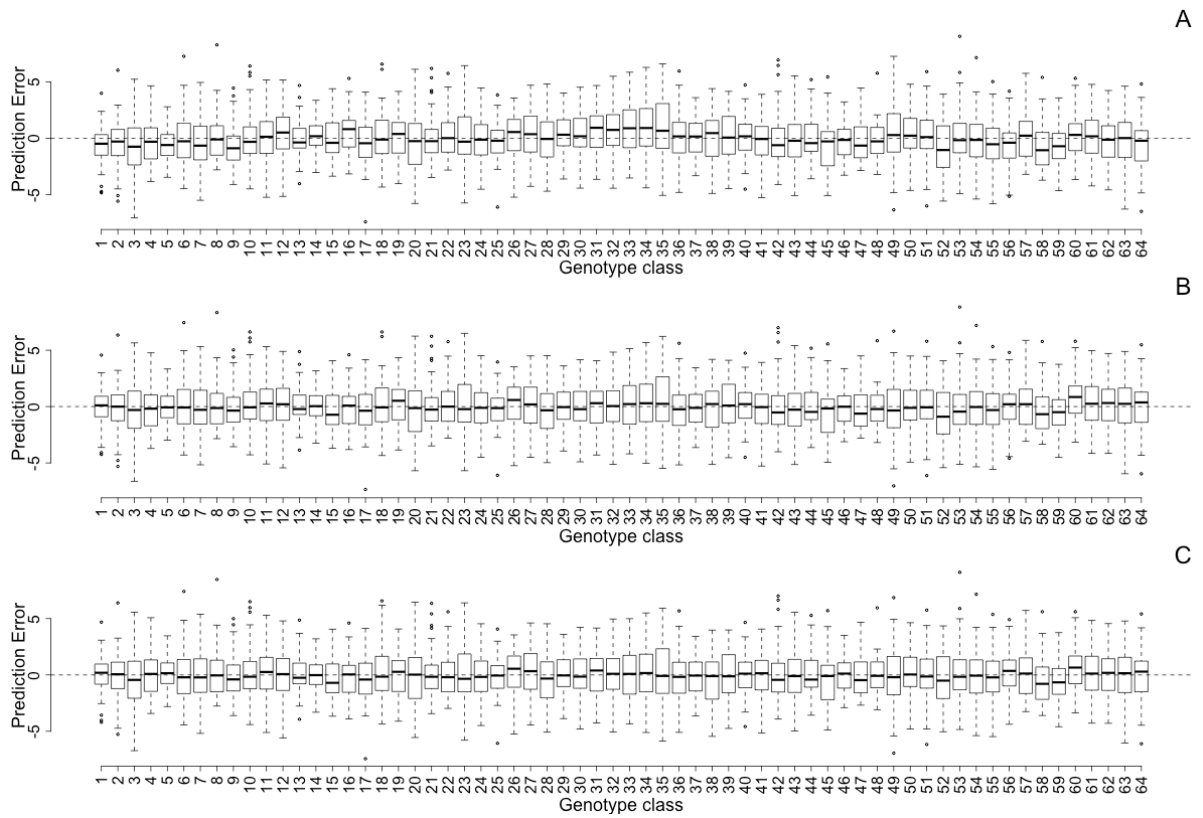


**Figure S15. Phenotypic prediction accuracy YPD.**

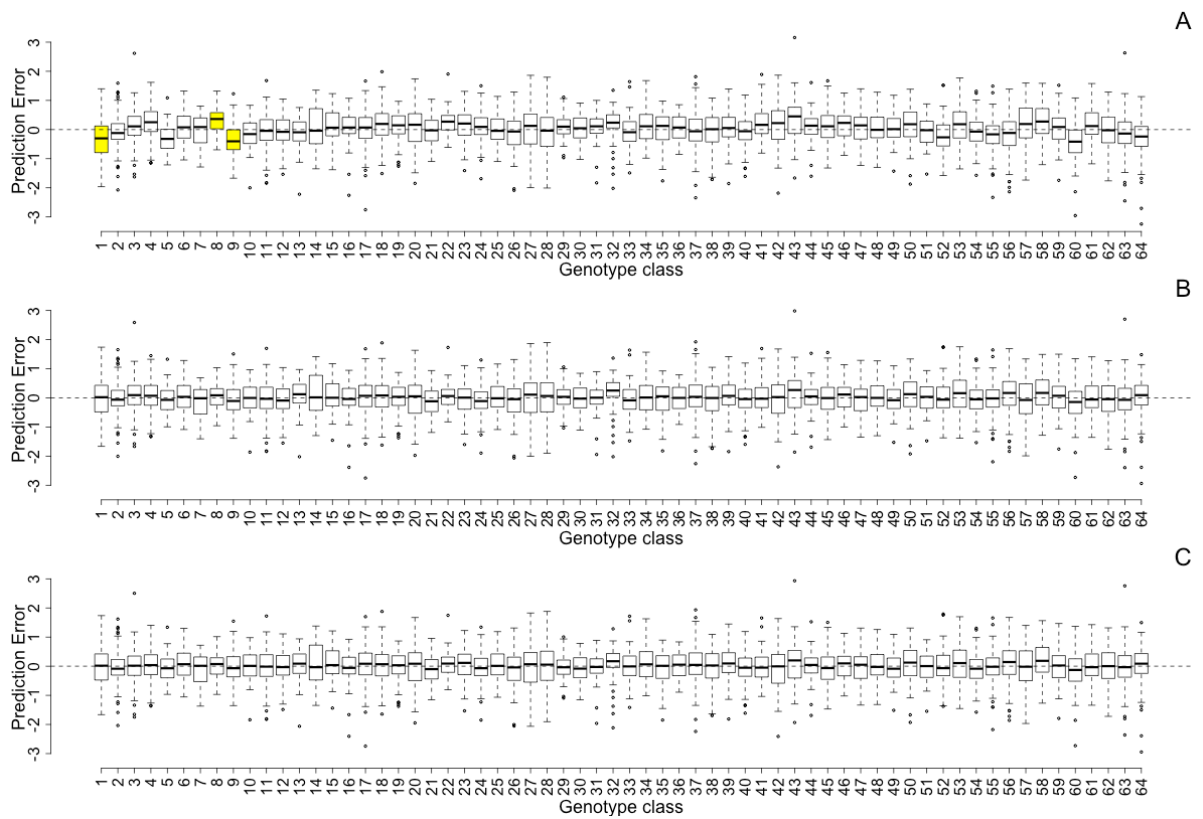


**Figure S16. Phenotypic prediction accuracy Xylose.**

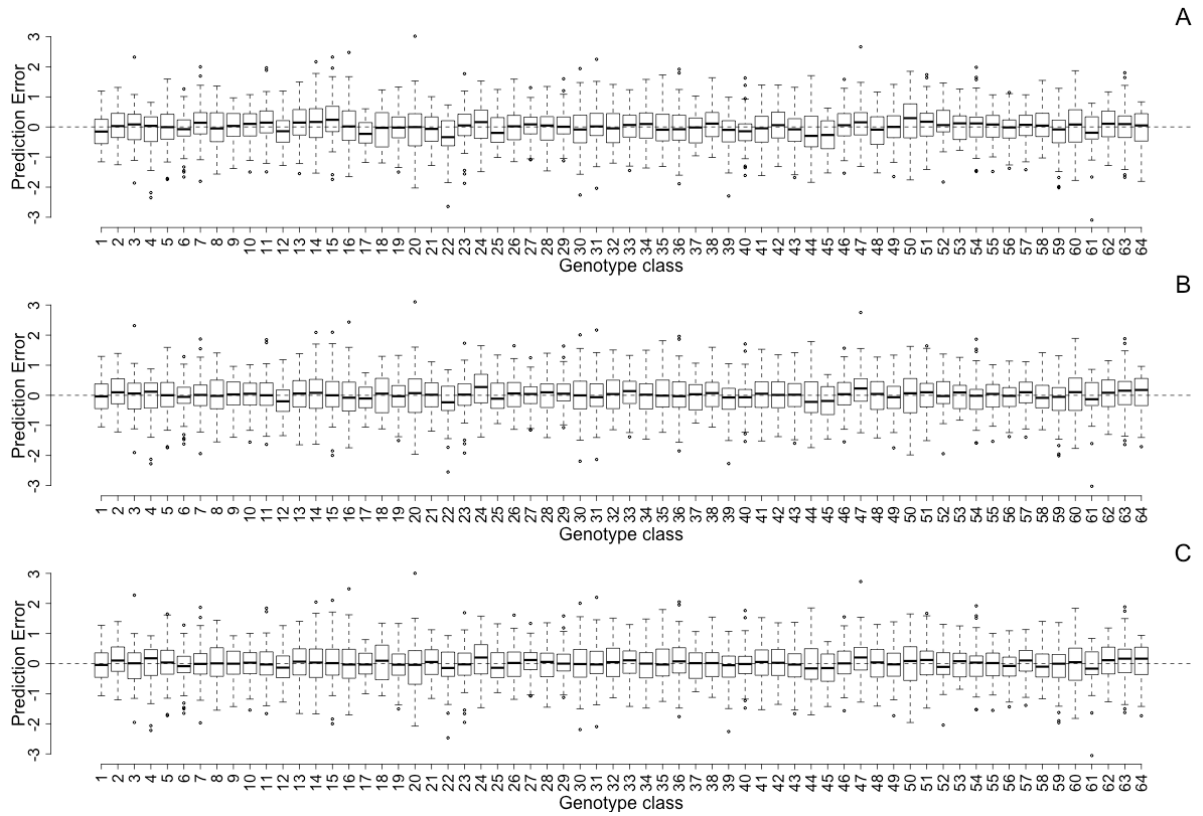


**Figure S17. Phenotypic prediction accuracy Raffinose.**

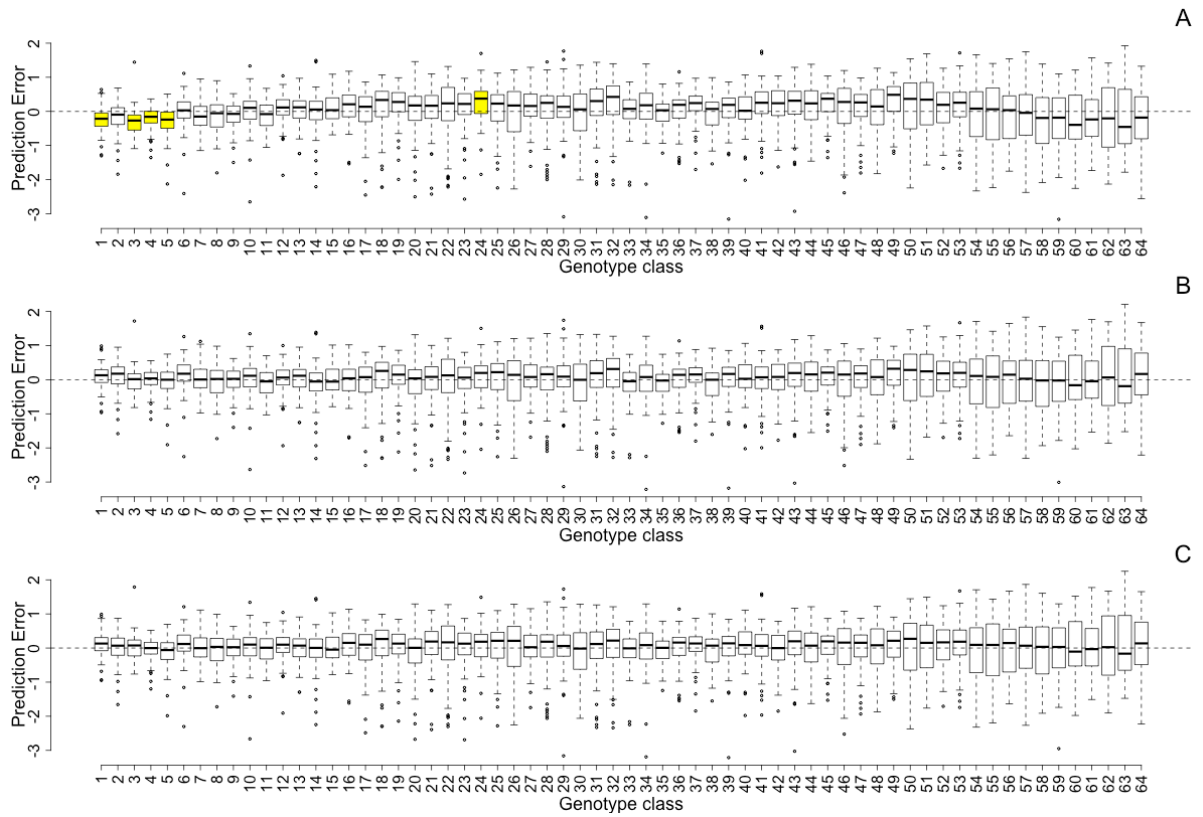


**Figure S18. Phenotypic prediction accuracy Neomycin, network 1.**

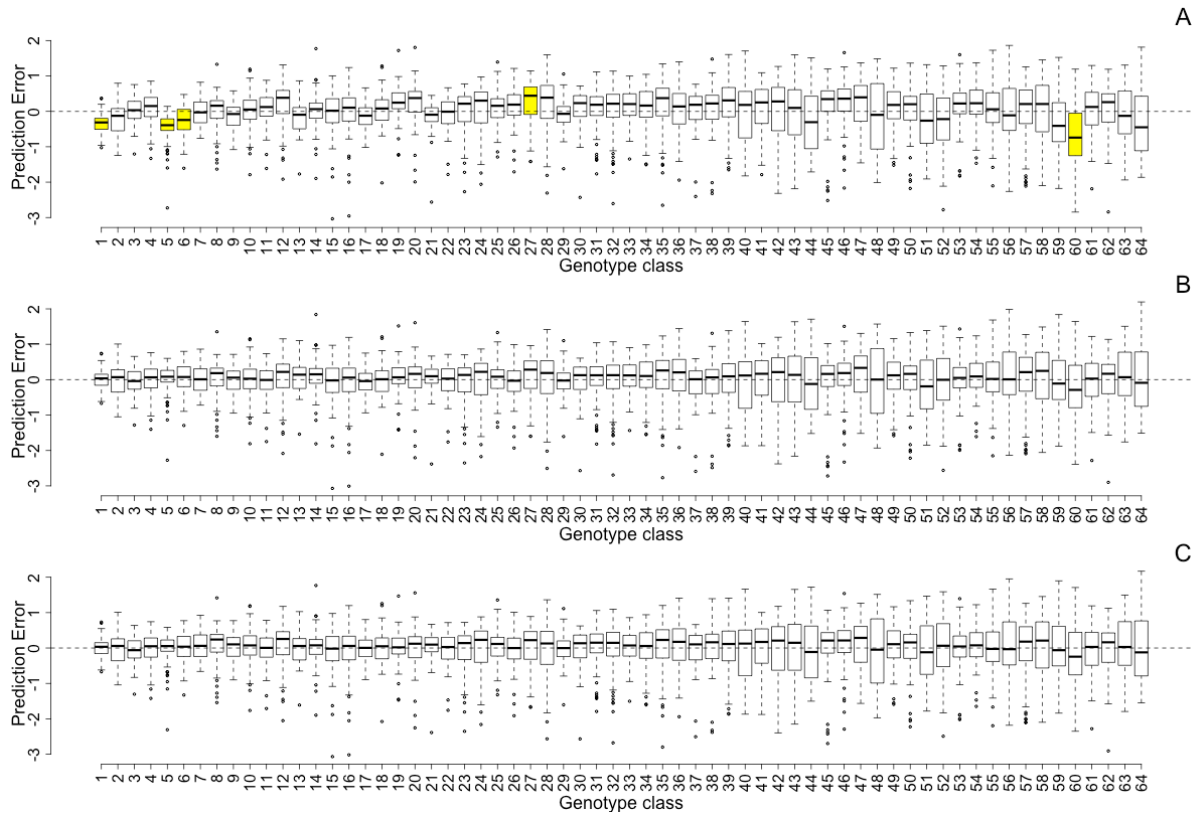


**Figure S19. Phenotypic prediction accuracy Neomycin, network 2.**

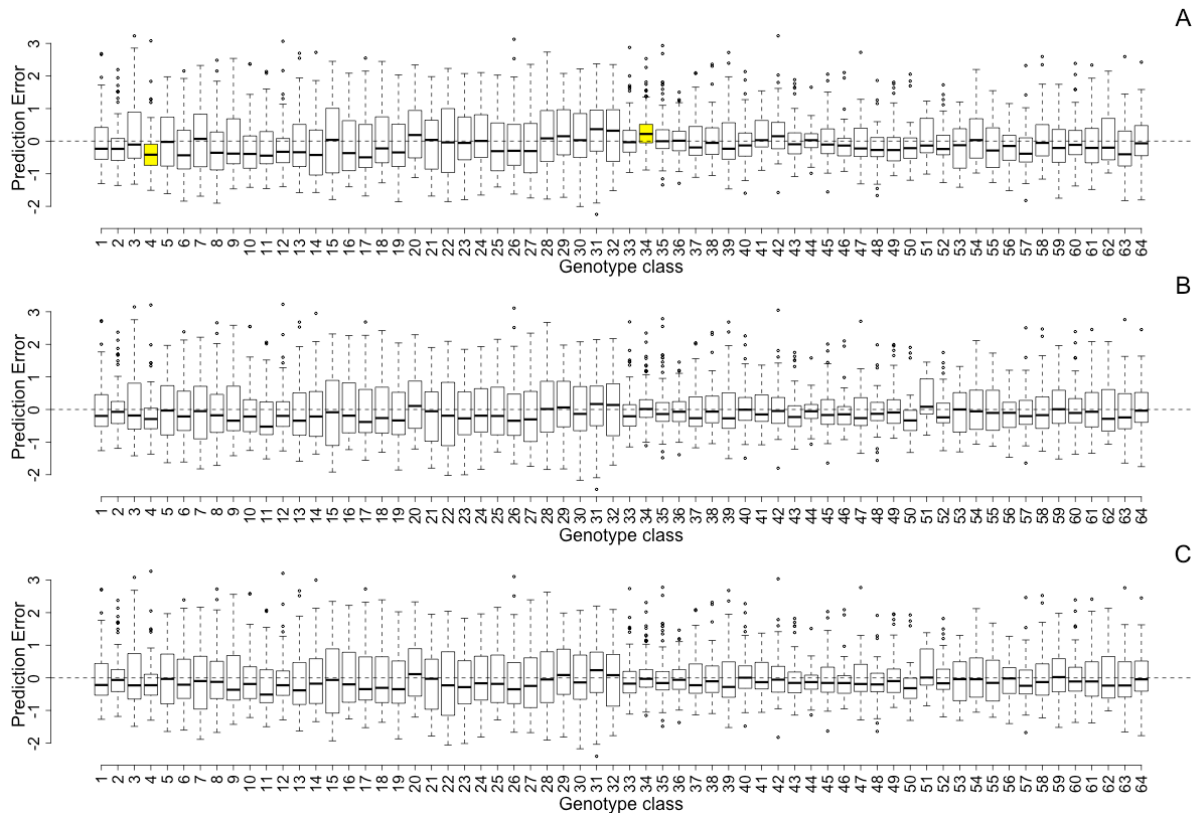


**Figure S19. Phenotypic prediction accuracy Manganese Sulfate, network 1.**

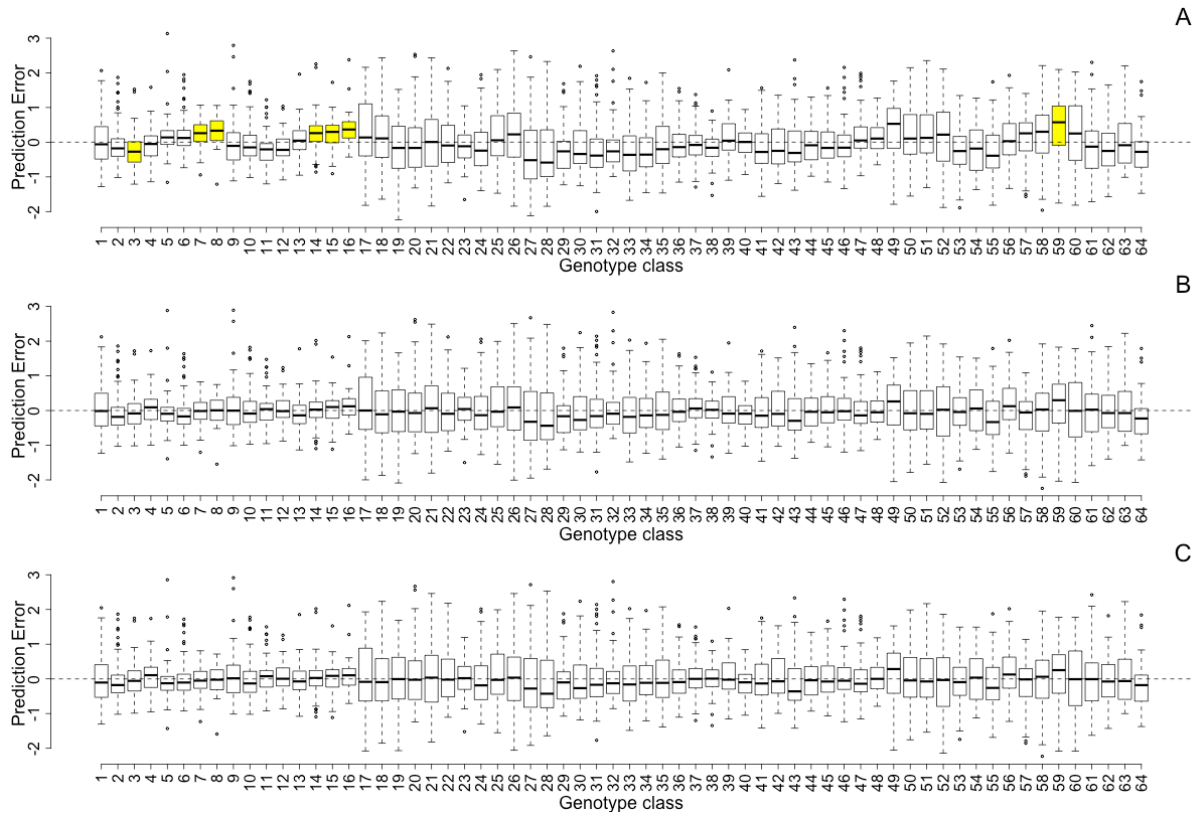


**Figure S20. Phenotypic prediction accuracy Manganese Sulfate, network 2.**

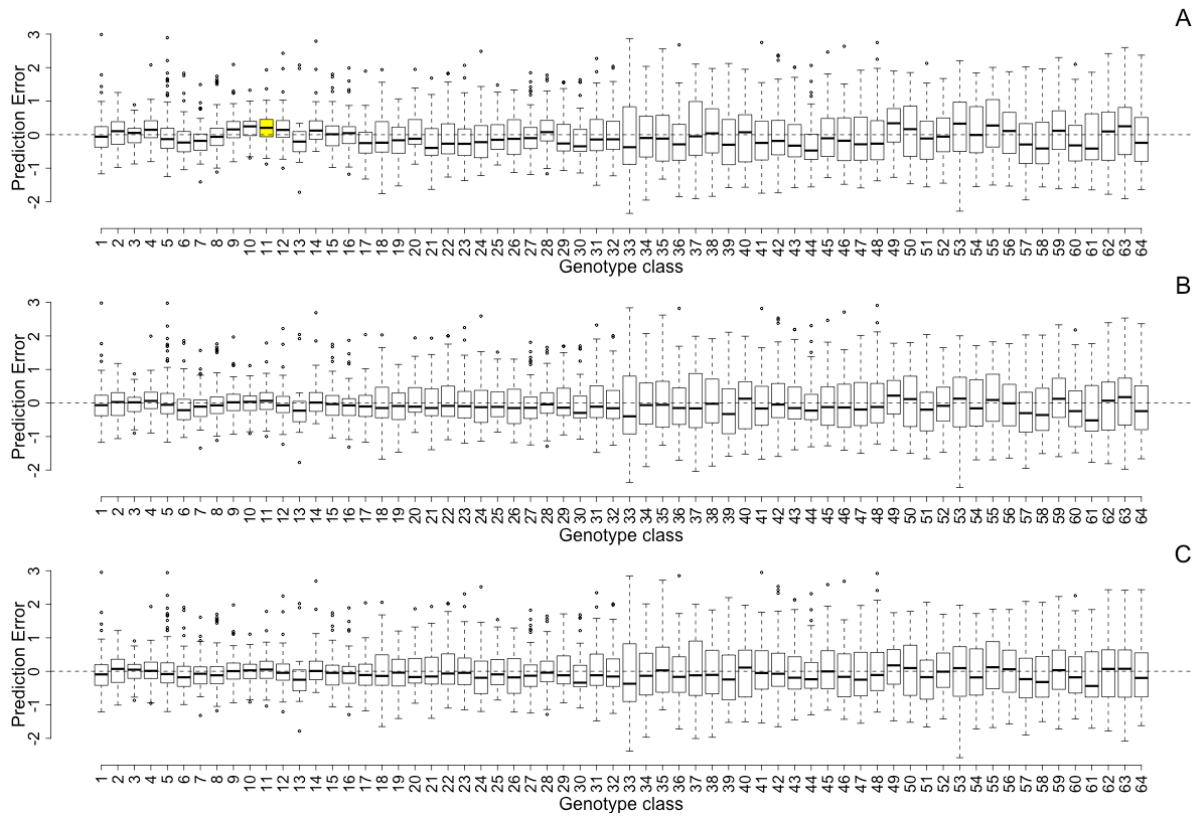


**Figure S21. Phenotypic prediction accuracy Manganese Sulfate, network 3.**

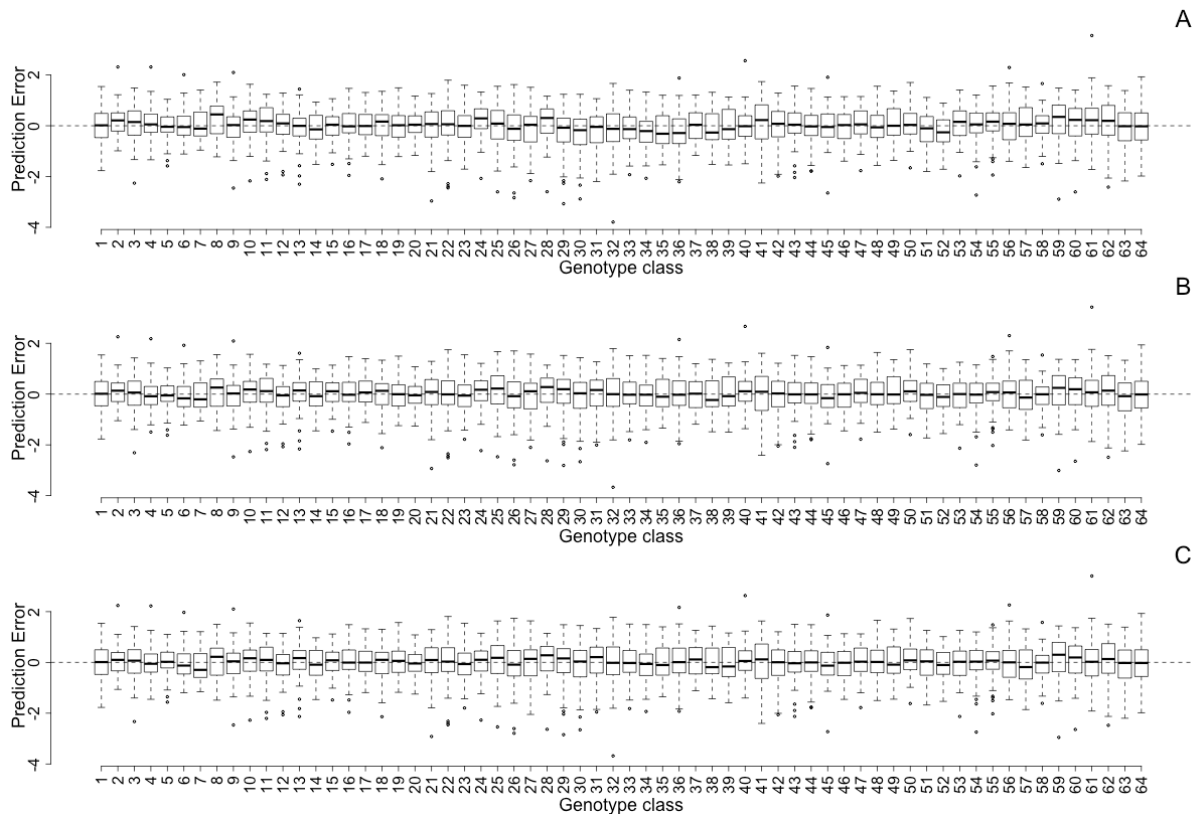


**Figure S22. Phenotypic prediction accuracy Lactate, network 1.**

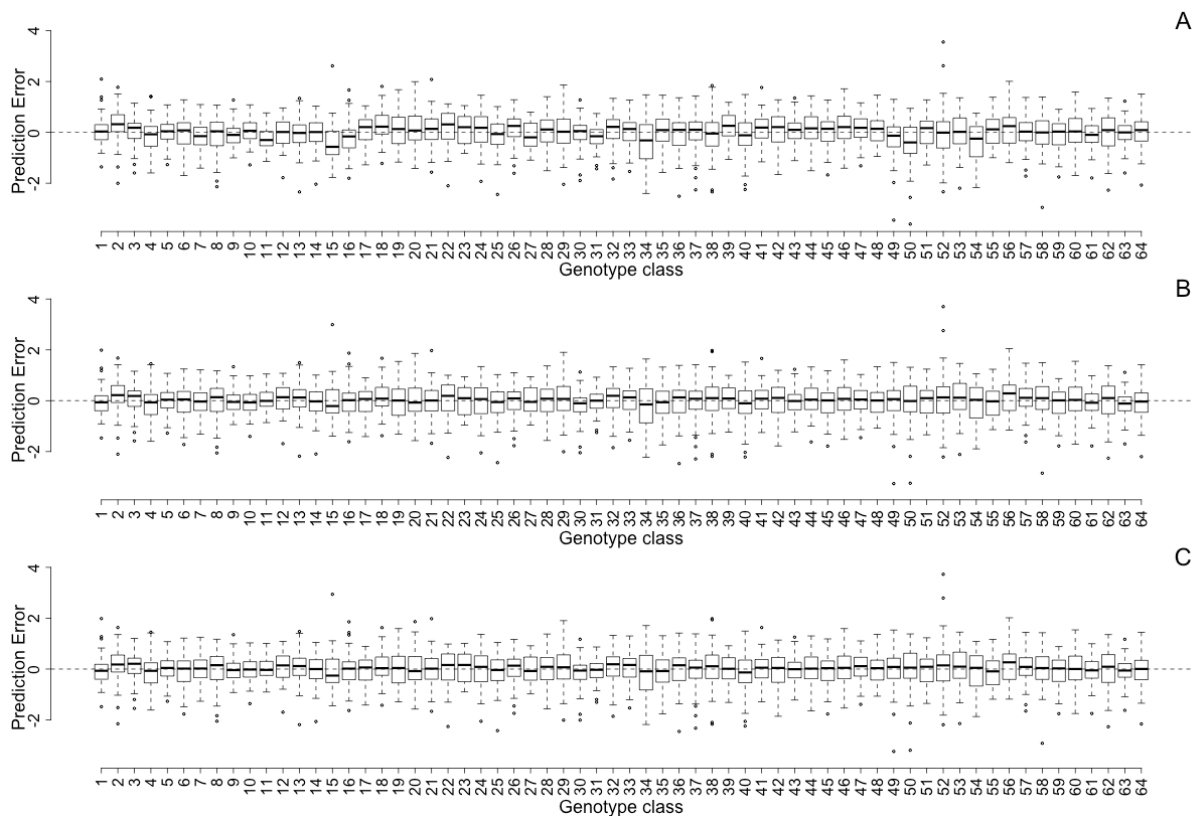


**Figure S23. Phenotypic prediction accuracy Lactate, network 2.**

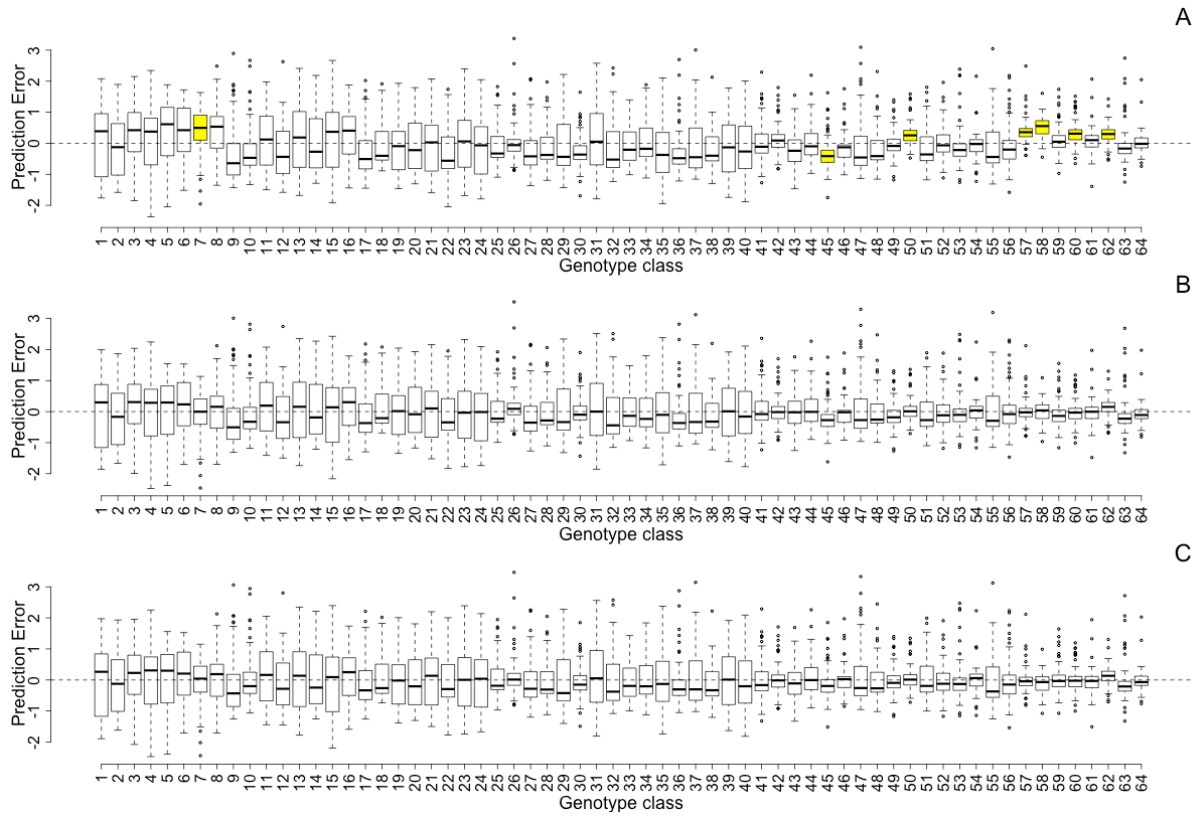


**Figure S24. Phenotypic prediction accuracy E6-Berbamine.**

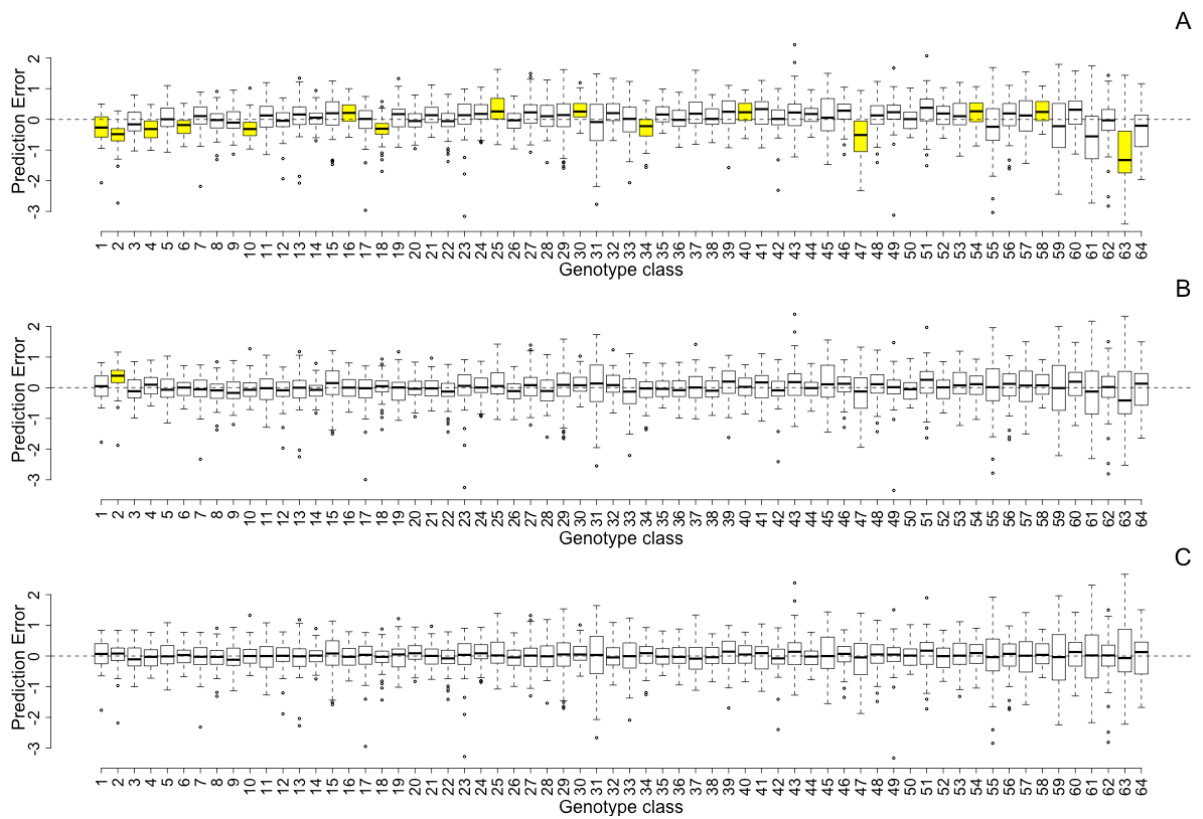


**Figure S25. Phenotypic prediction accuracy Copper Sulfate.**

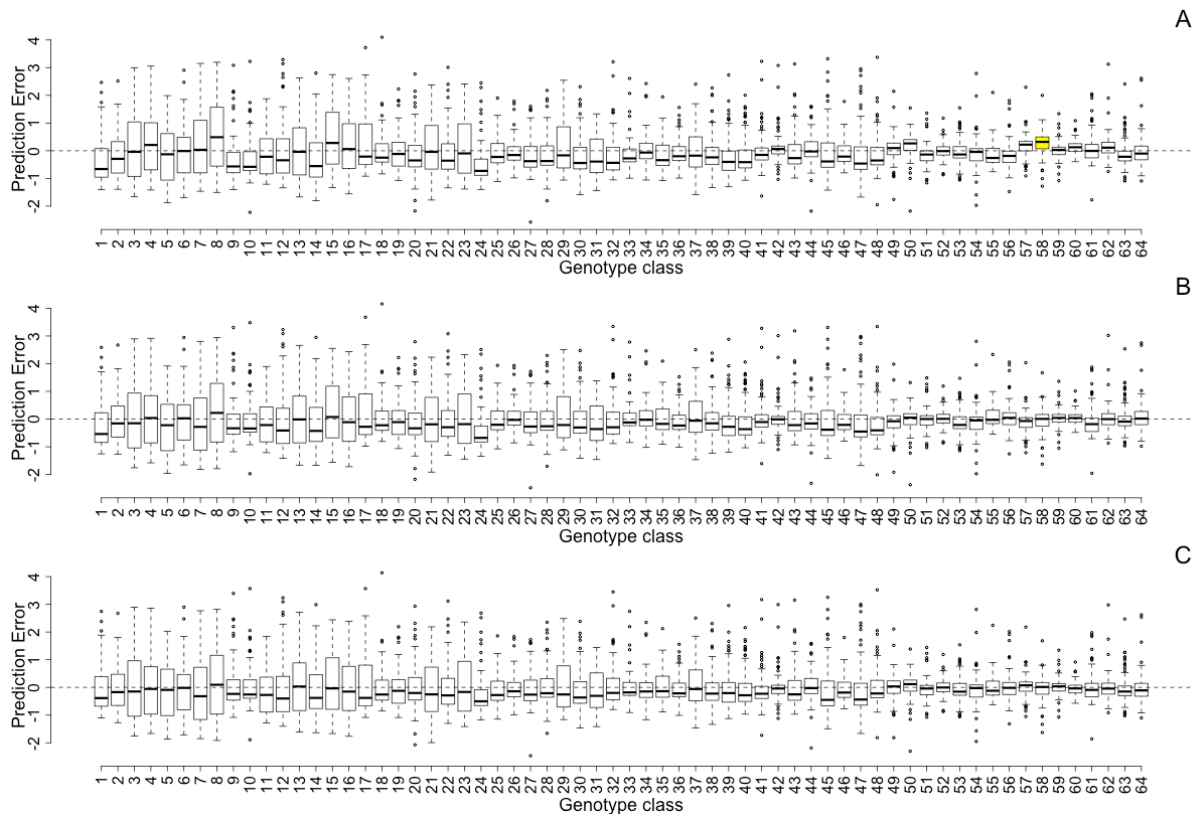


**Figure S26. Phenotypic prediction accuracy Cobalt Chloride.**

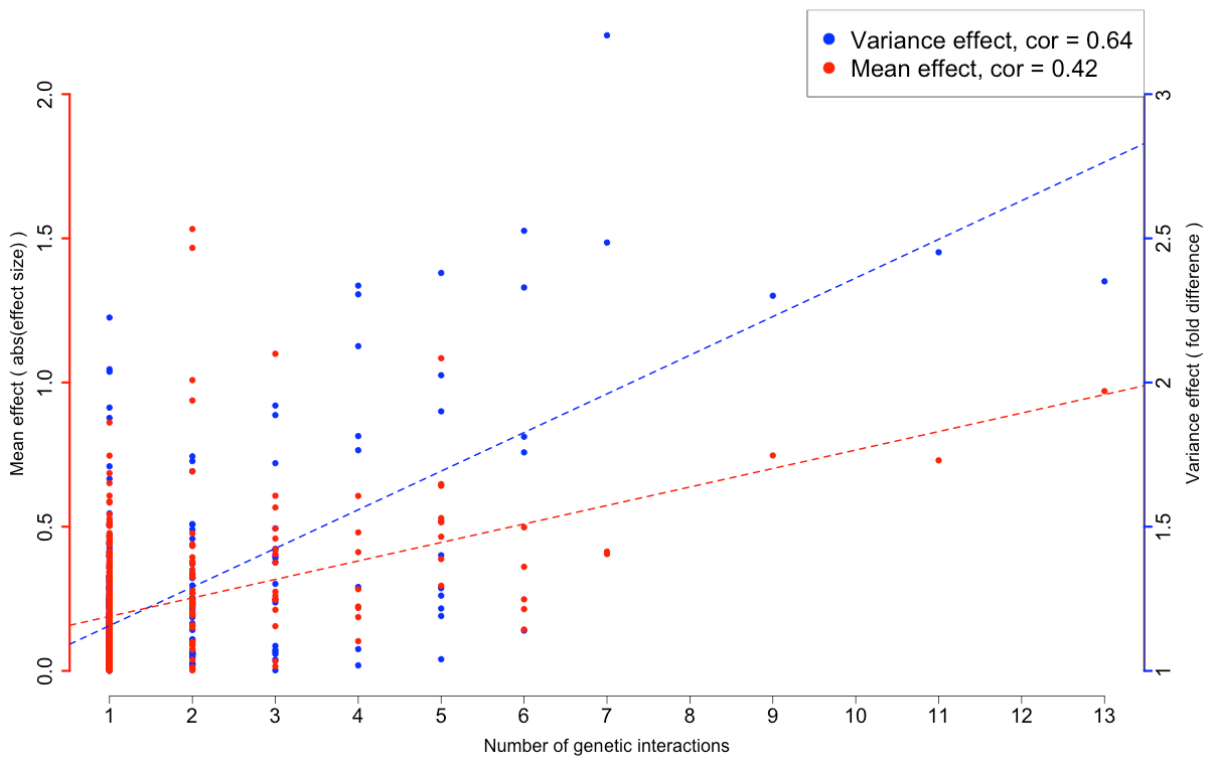


**Figure S27. Correlation between number of genetic interactions and marginal phenotypic effect.** Each point represents one locus. The X-axis show the number of pairwise genetic interactions each locus is involved in and the Y-axes shows their marginal effect on the phenotype. The red points show the marginal effect on the mean of the phenotype (cor = 0.42,

$p < 1 \times 10^{-12}$ ), whereas the blue points show the effect on the phenotypic variance ( $cor = 0.64$ ,  $p < 1 \times 10^{-12}$ ).

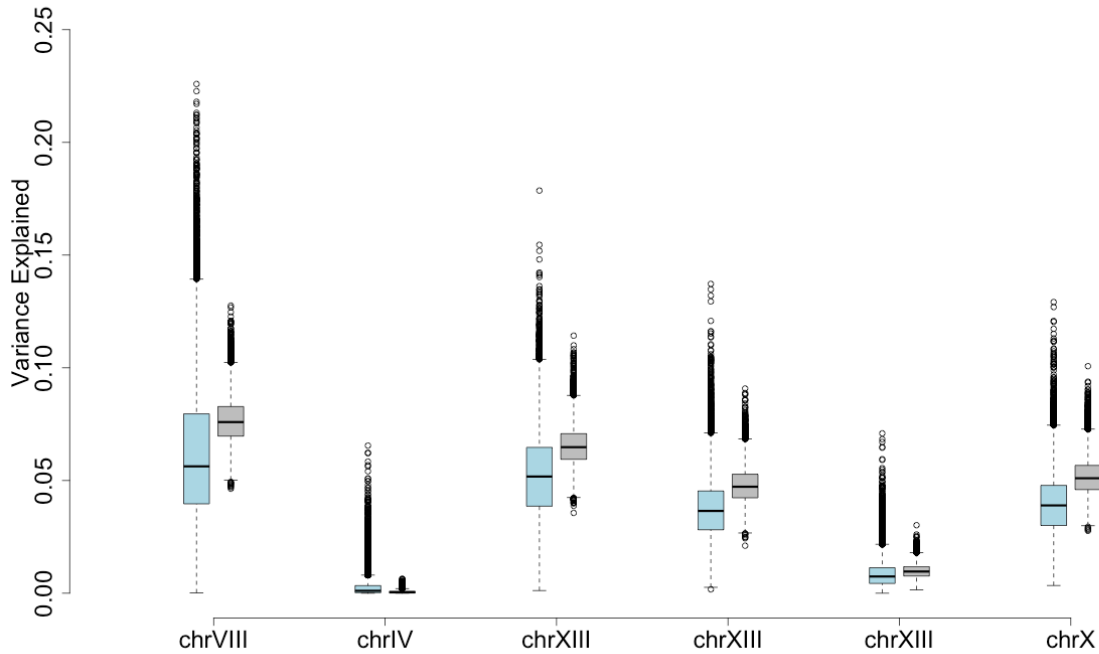


**Figure S28. Phenotypic variance explained across simulated populations, Zeocin.** Boxplots illustrating how the additive genetic variances explained by each of the six loci in the network depend on the allele frequencies at the other loci. The distributions are obtained using simulations where the additive genetic variances are estimated for the loci at a fixed allele frequency 0.5, while varying the frequencies at the other 5 loci from 0.05 to 0.95. The light blue boxes represent the variability in the additive genetic variances when simulating populations based on the observed phenotypic means for the allelic combinations in the networks and the grey boxes when simulating based on the phenotypic means predicted using an additive genetic model. Results are represented in the same manner in figures S29-S41.



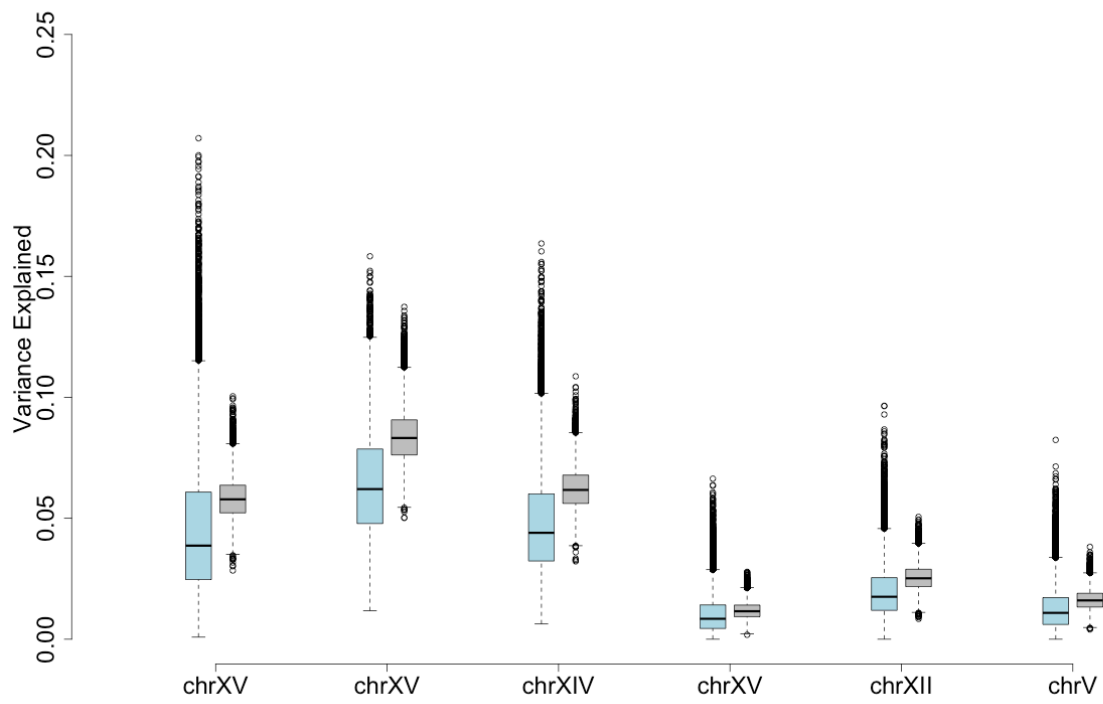


**Figure S29. Phenotypic variance explained across simulated populations, YPD.**

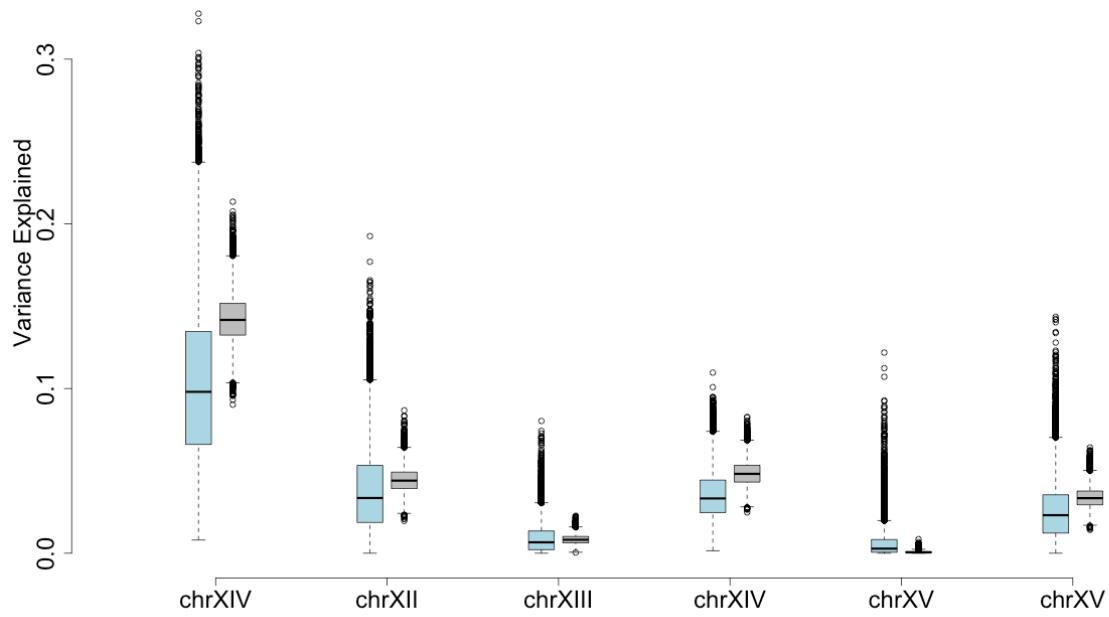


**Figure S30. Phenotypic variance explained across simulated populations, Xylose.**

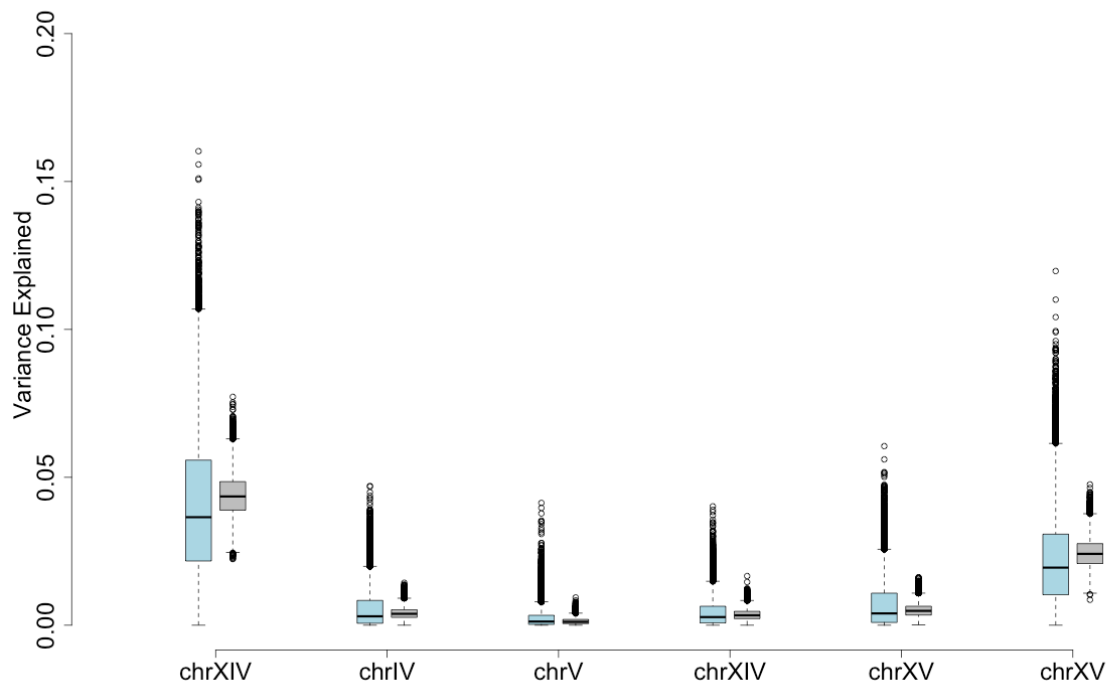


**Figure S31. Phenotypic variance explained across simulated populations, Raffinose.**

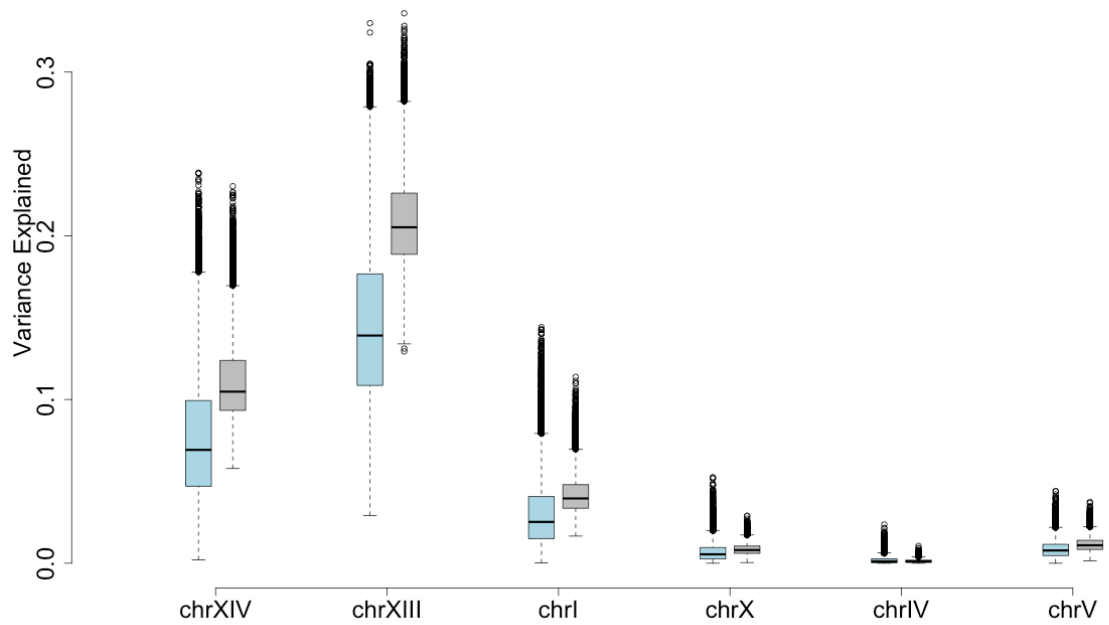


**Figure S32. Phenotypic variance explained across simulated populations, Neomycin network 1.**

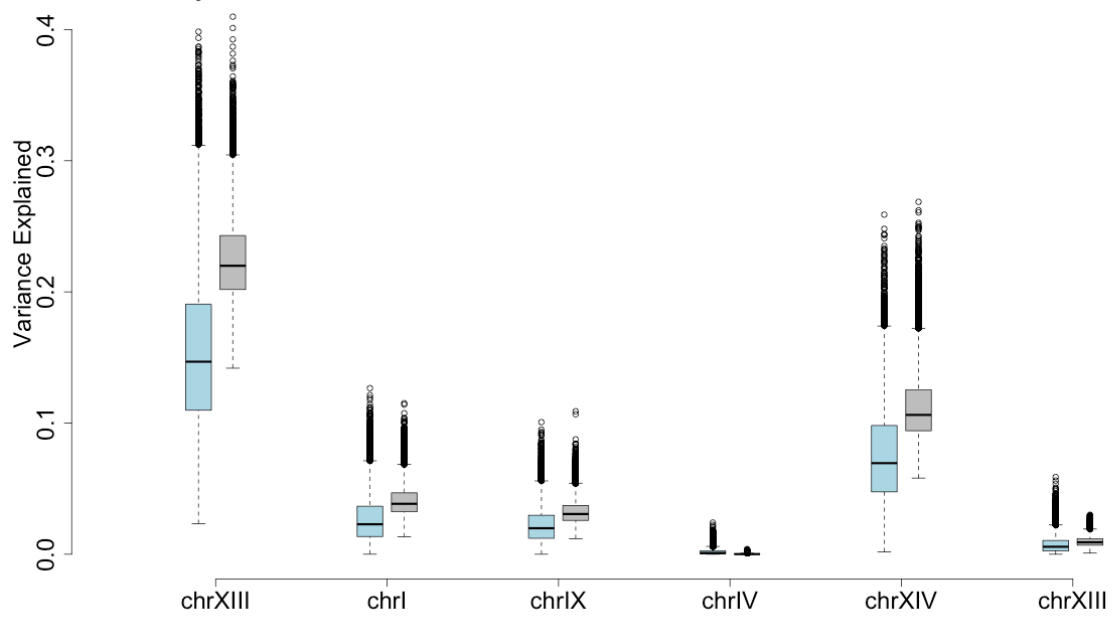


**Figure S33. Phenotypic variance explained across simulated populations, Neomycin network 2.**

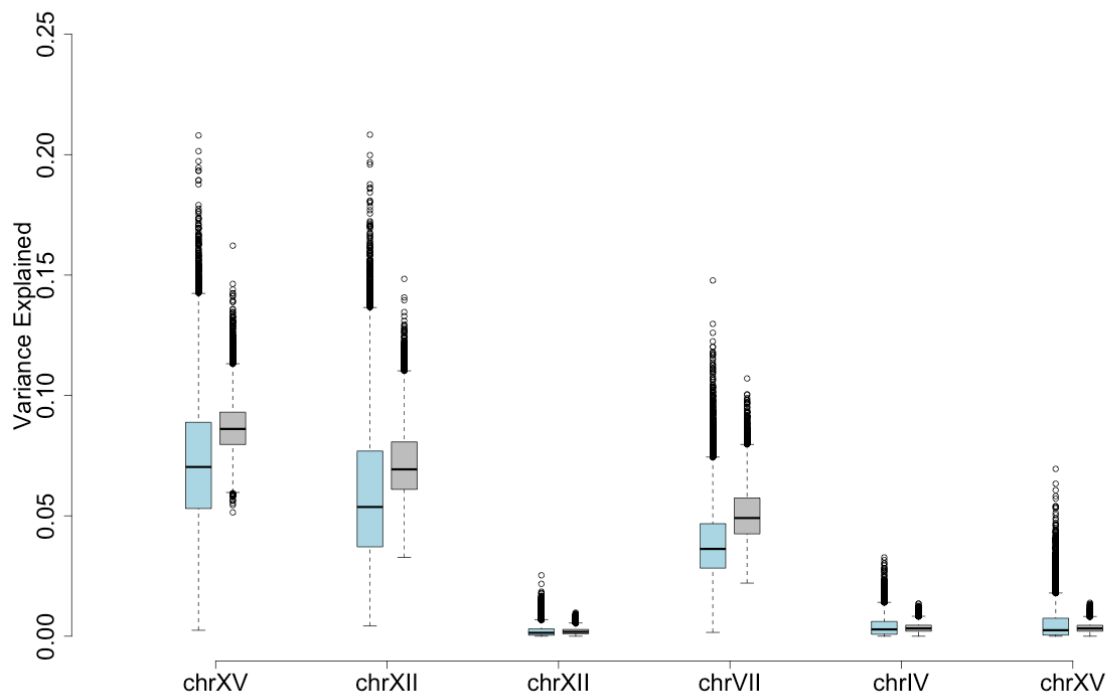


**Figure S34. Phenotypic variance explained across simulated populations, Manganese Sulfate network 1.**

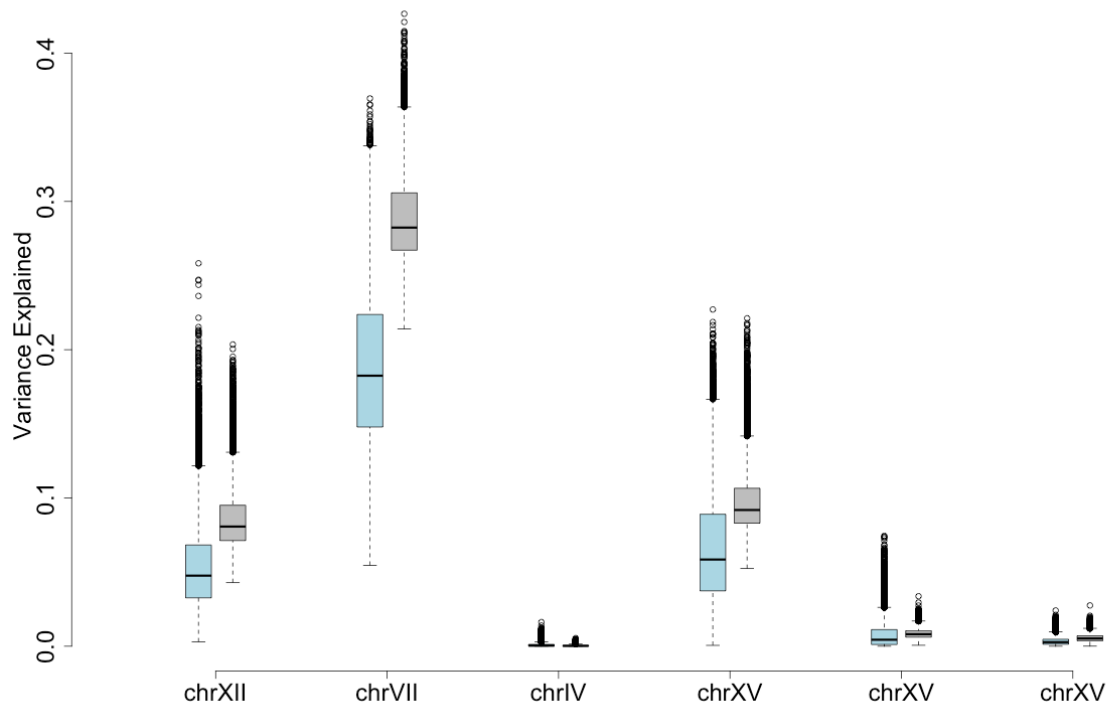


**Figure S35. Phenotypic variance explained across simulated populations, Manganese Sulfate network 2.**

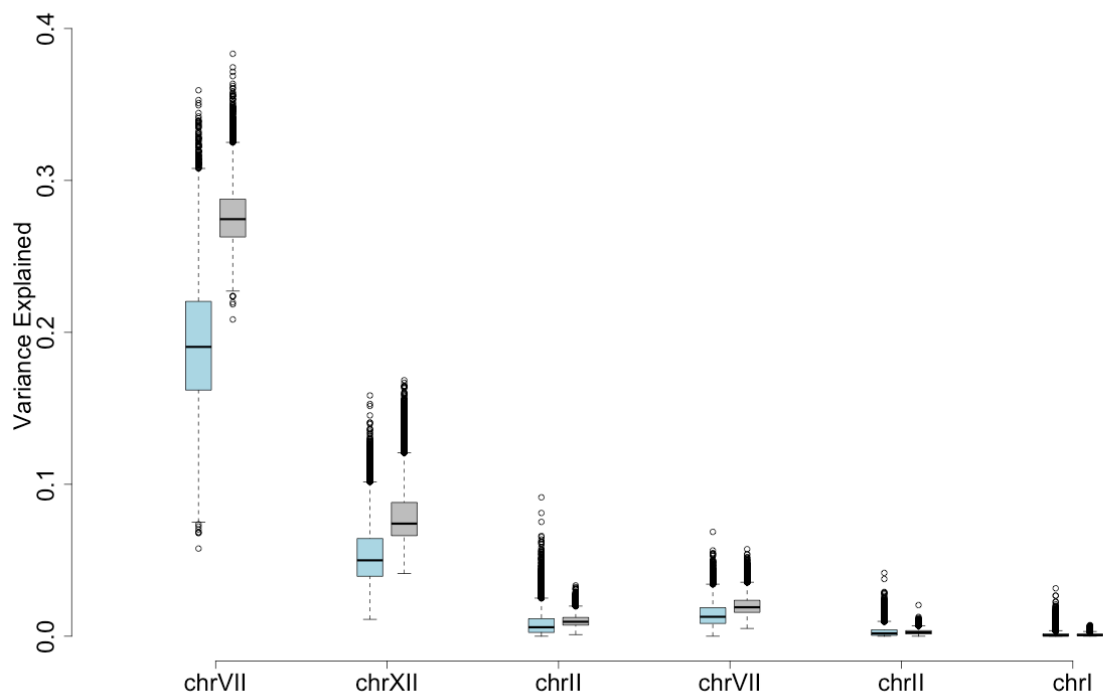


**Figure S36. Phenotypic variance explained across simulated populations, Manganese Sulfate network 3.**

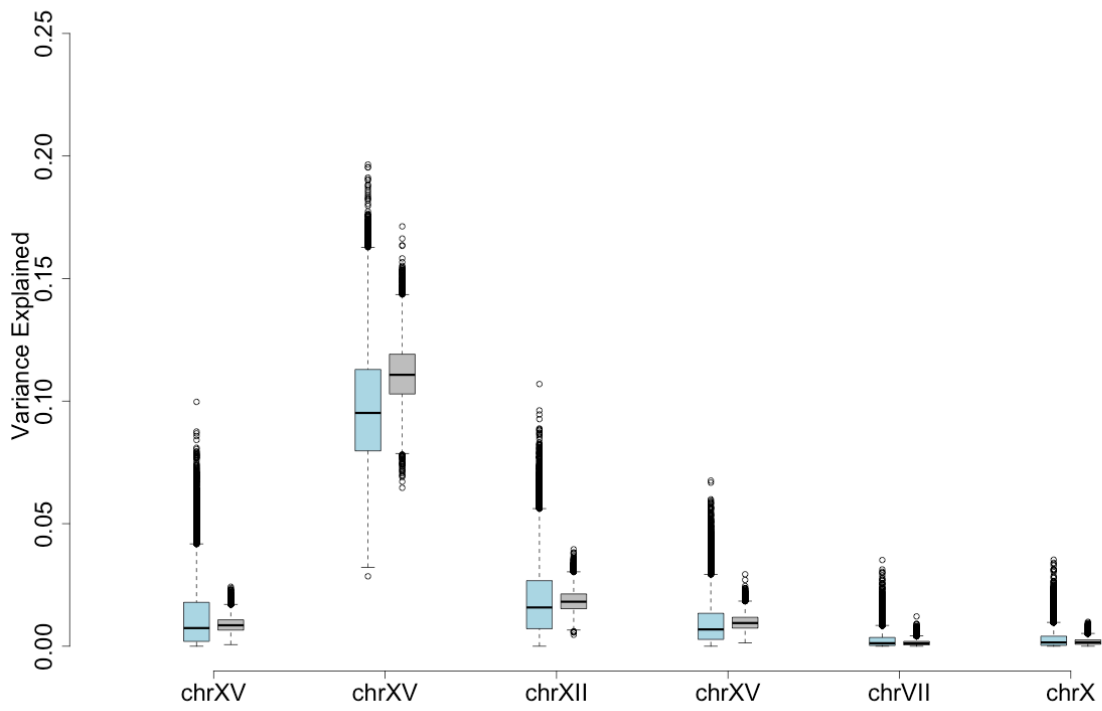


**Figure S37. Phenotypic variance explained across simulated populations, Lactate network 1.**

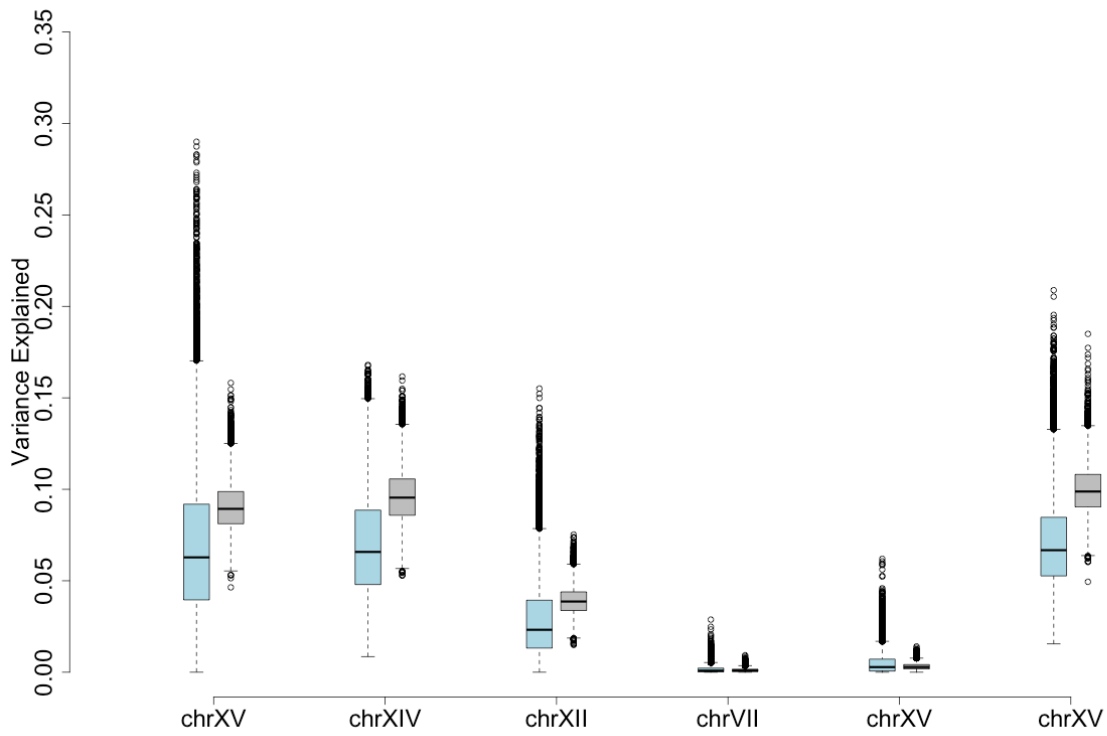


**Figure S38. Phenotypic variance explained across simulated populations, Lactate network 2.**

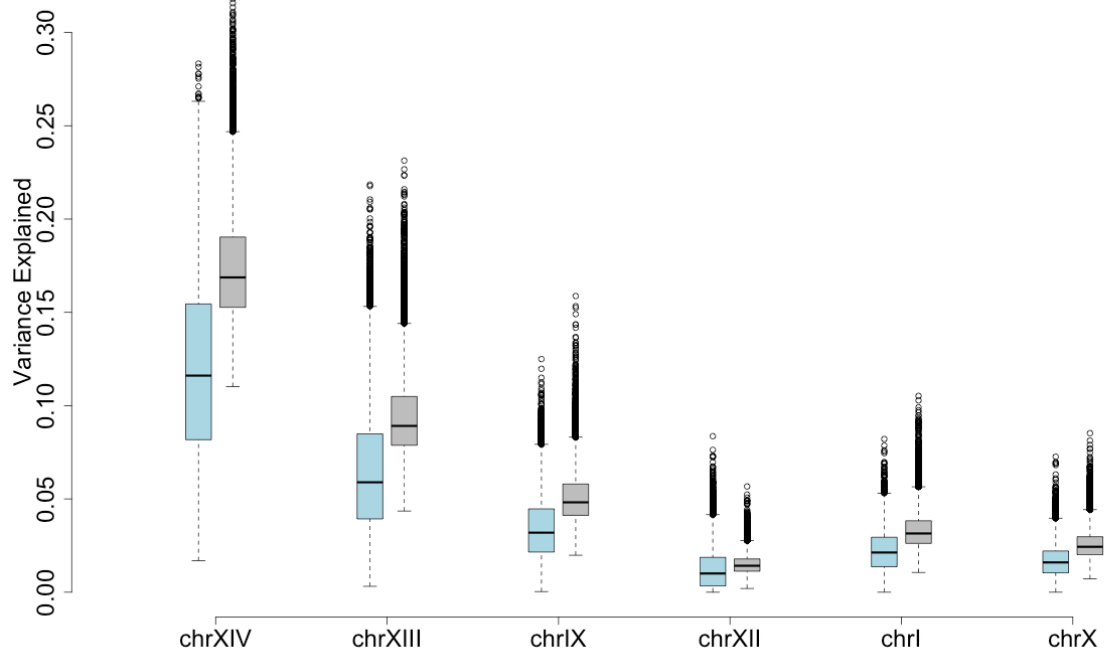


**Figure S39.** Phenotypic variance explained across simulated populations, E6-Berberine.

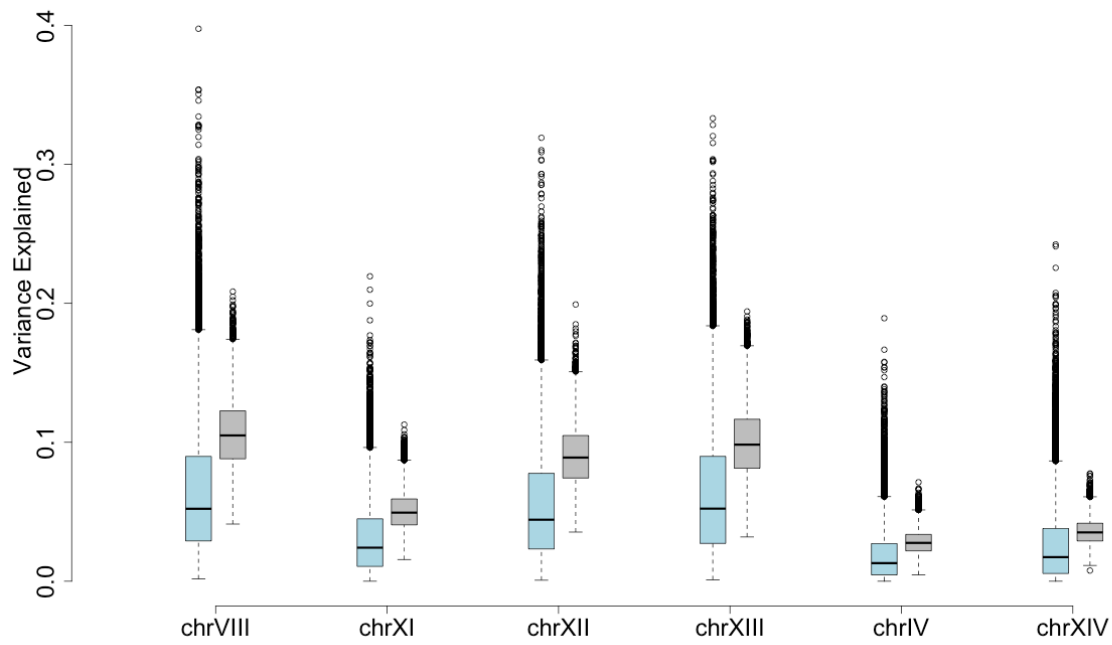


**Figure S40.** Phenotypic variance explained across simulated populations, Copper Sulfate.

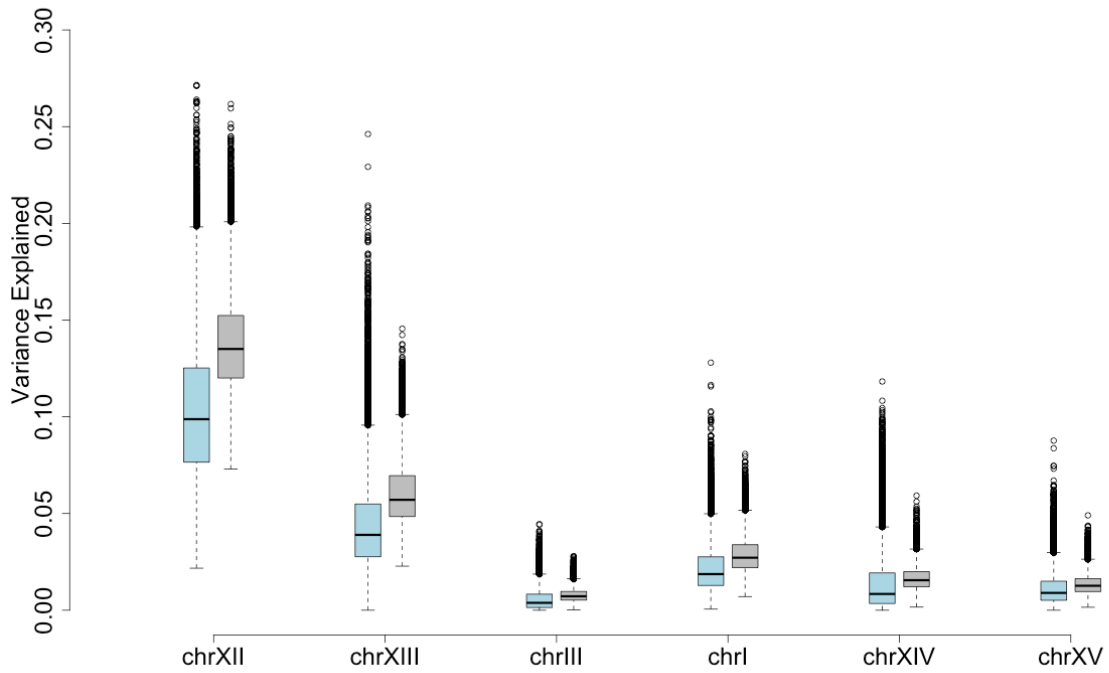


**Figure S41. Phenotypic variance explained across simulated populations, Cobalt Chloride.**

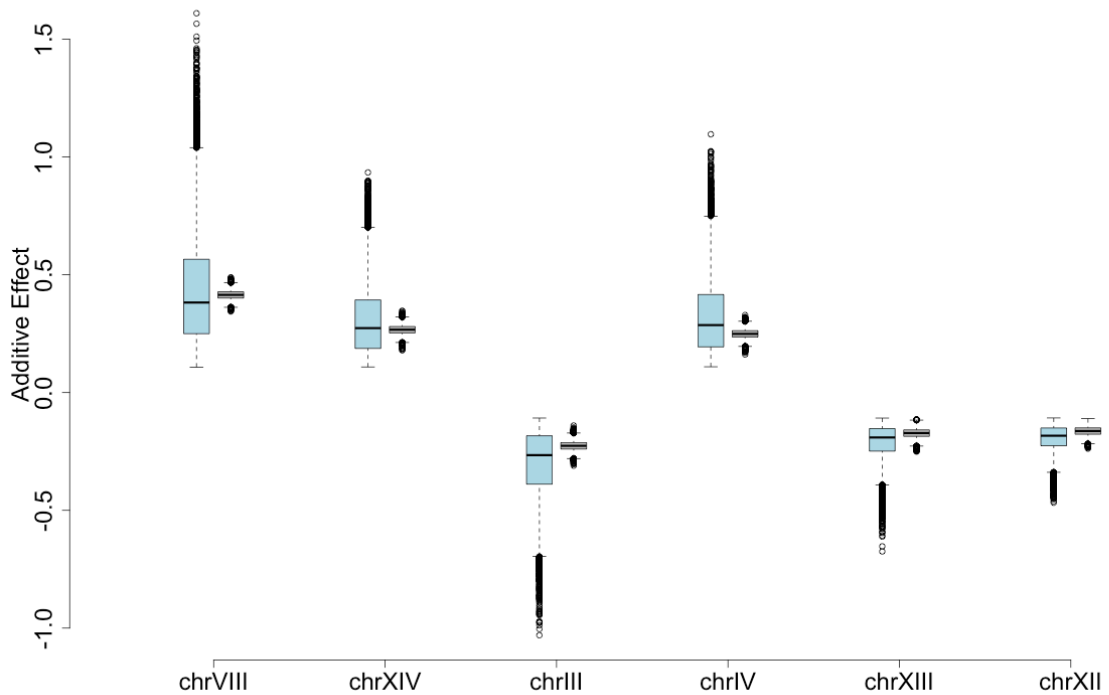


**Figure S42. Additive phenotypic effect across simulated populations, Indole Acetic Acid.** Boxplots illustrating how the additive (marginal) phenotypic effects of each of the six loci in the network depend on the allele frequencies at the other loci. The distributions are obtained using simulations where the additive effects are estimated for the loci at a fixed allele

frequency 0.5, while varying the frequencies at the other 5 loci from 0.05 to 0.95. The light blue boxes represent the variability in the additive effects when simulating populations based on the observed phenotypic means for the allelic combinations in the networks and the grey boxes when simulating based on the phenotypic means predicted using an additive genetic model. Results are represented in the same manner in figures S42-S41.

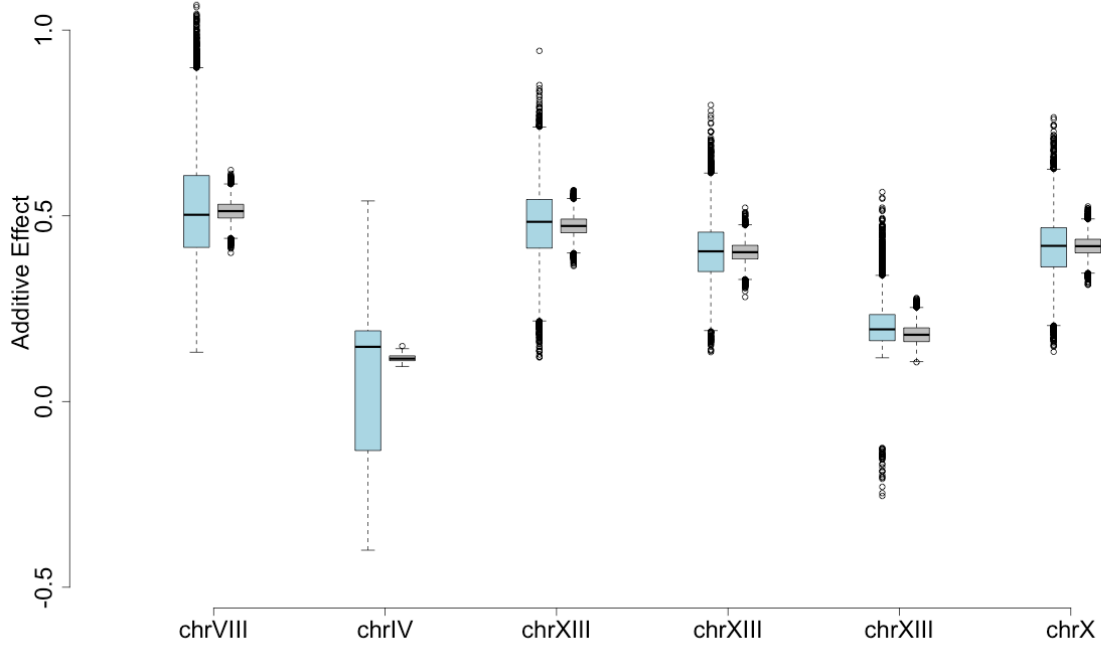


**Figure S43. Additive phenotypic effect across simulated populations, Zeocin.**



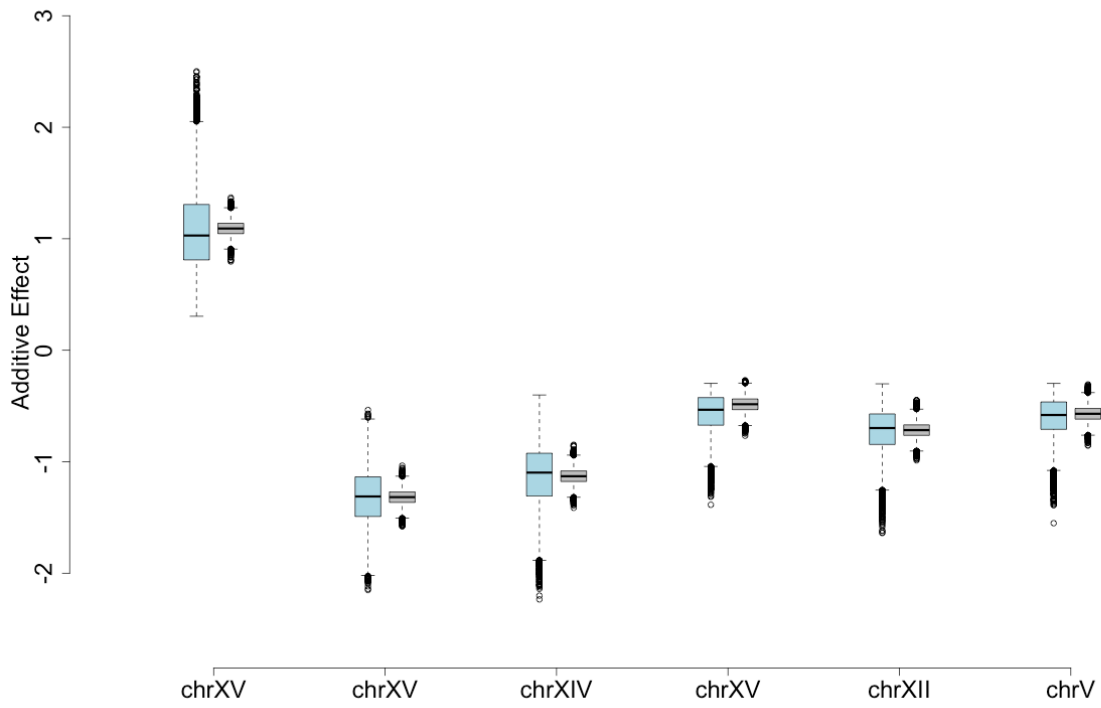


**Figure S44. Additive phenotypic effect across simulated populations, YPD.**

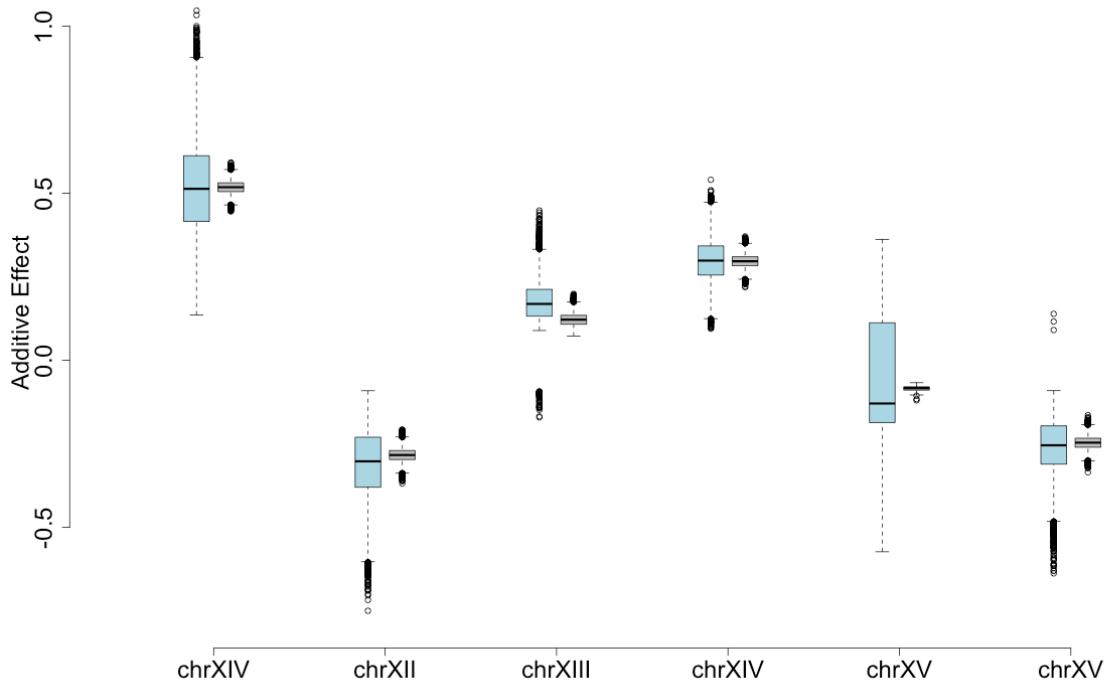


**Figure S45. Additive phenotypic effect across simulated populations, Xylose.**

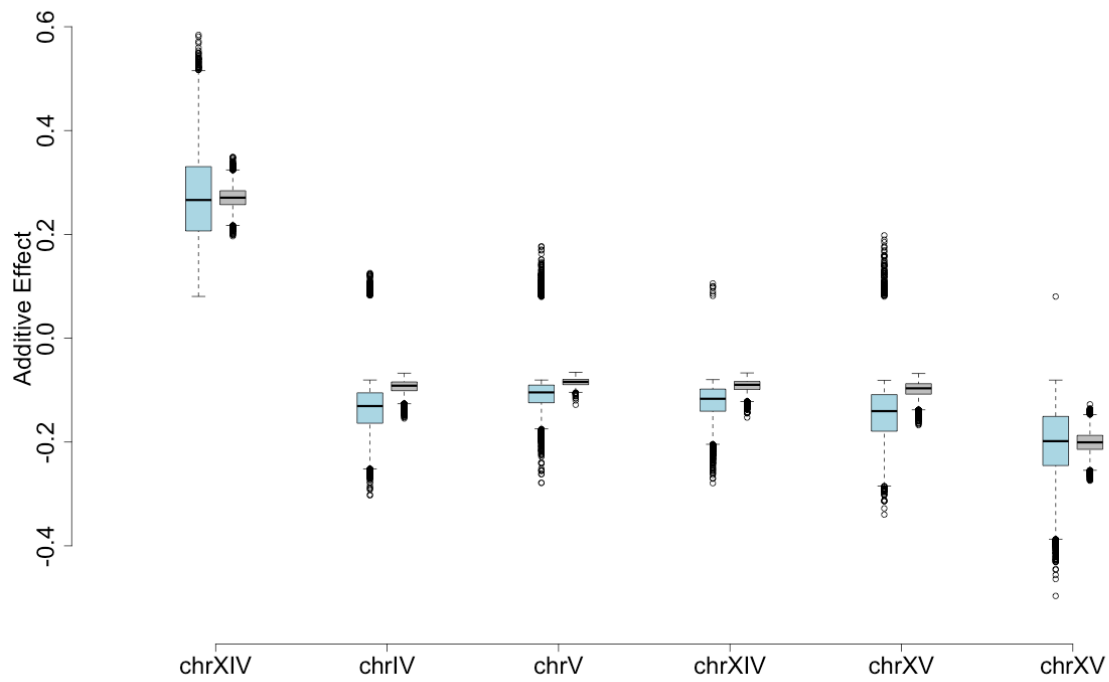


**Figure S46. Additive phenotypic effect across simulated populations, Raffinose.**

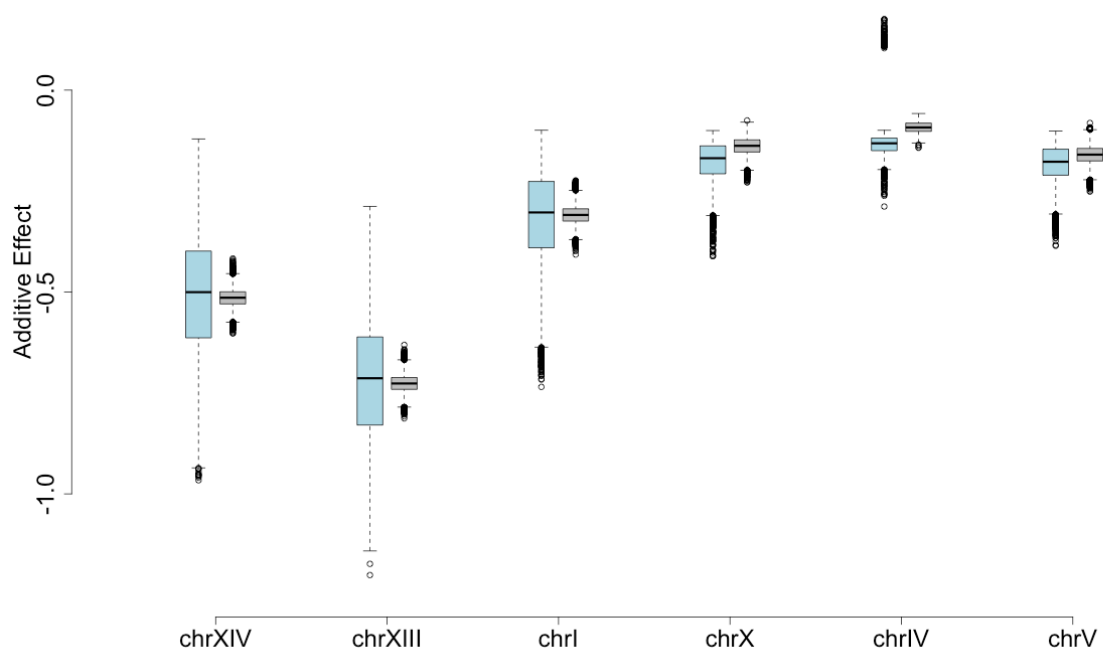


**Figure S47. Additive phenotypic effect across simulated populations, Neomycin network 1.**

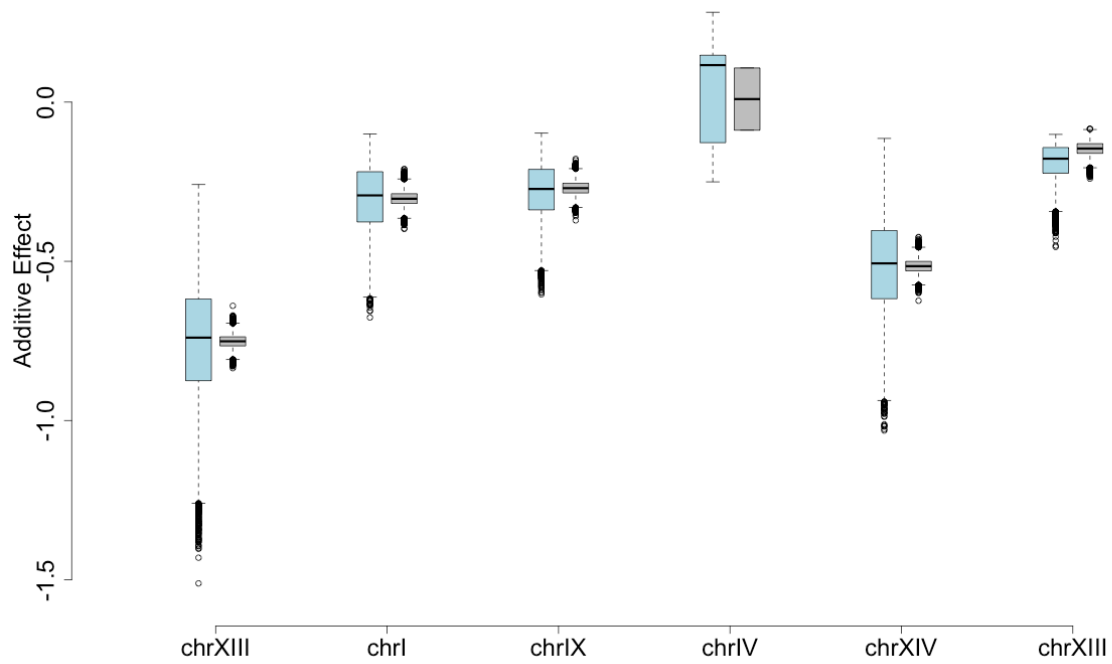


**Figure S48.** Additive phenotypic effect across simulated populations, Neomycin network 2.

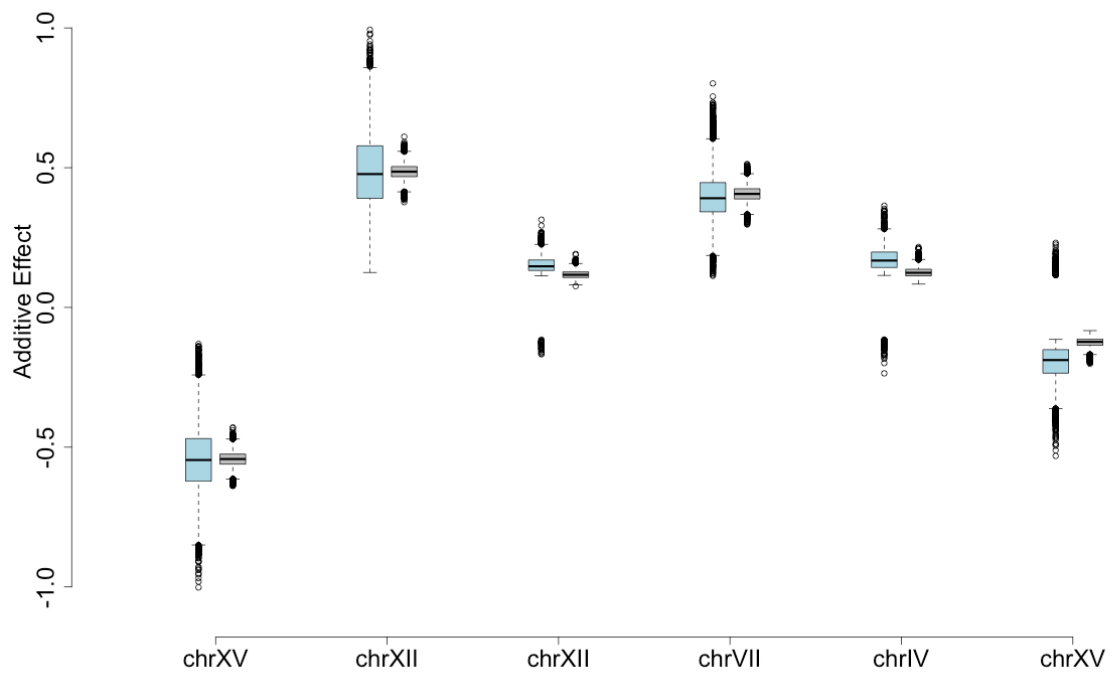


**Figure S49.** Additive phenotypic effect across simulated populations, Manganese Sulfate network 1.

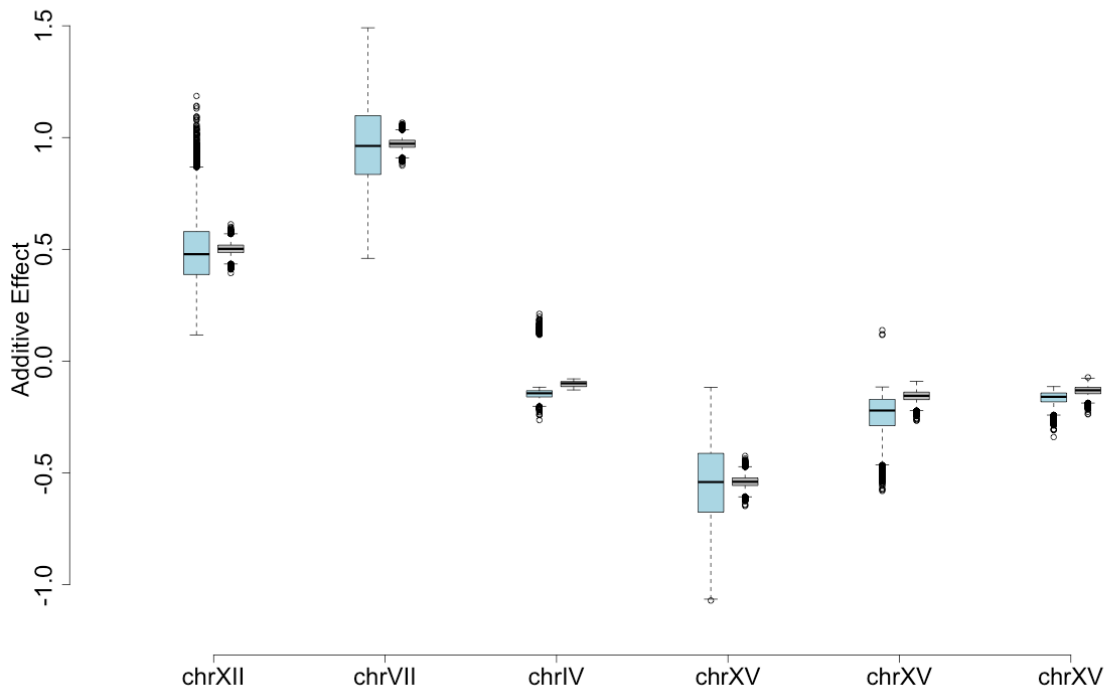


**Figure S50.** Additive phenotypic effect across simulated populations, Manganese Sulfate network 2.

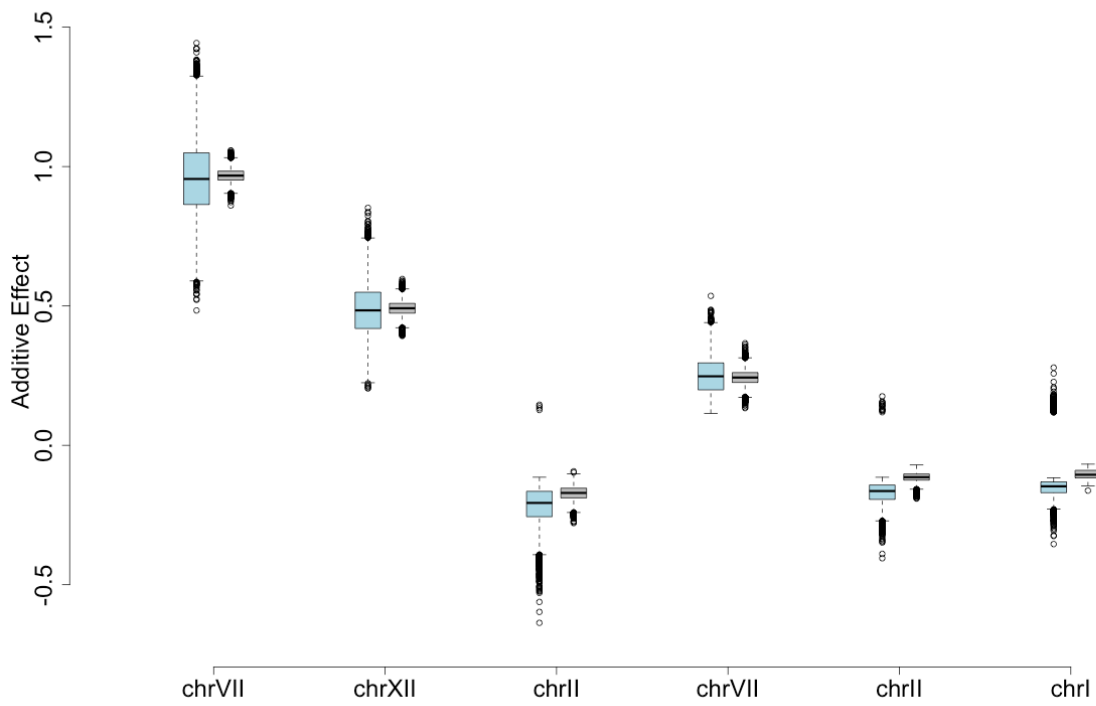


**Figure S51.** Additive phenotypic effect across simulated populations, Manganese Sulfate network 3.

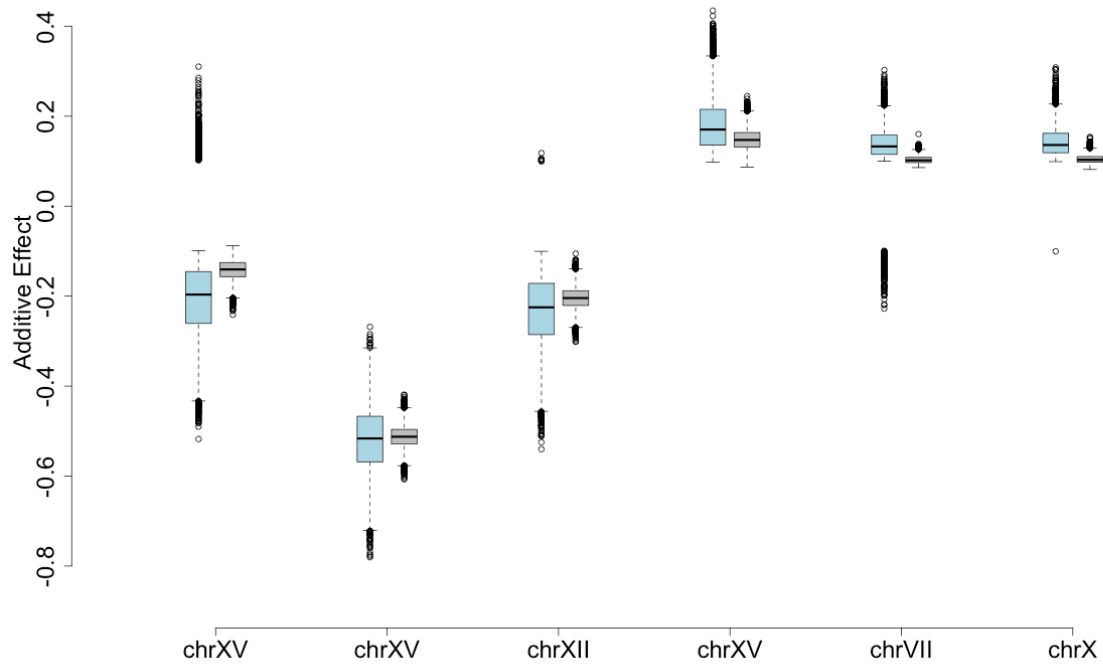


**Figure S52. Additive phenotypic effect across simulated populations, Lactate network 1.**

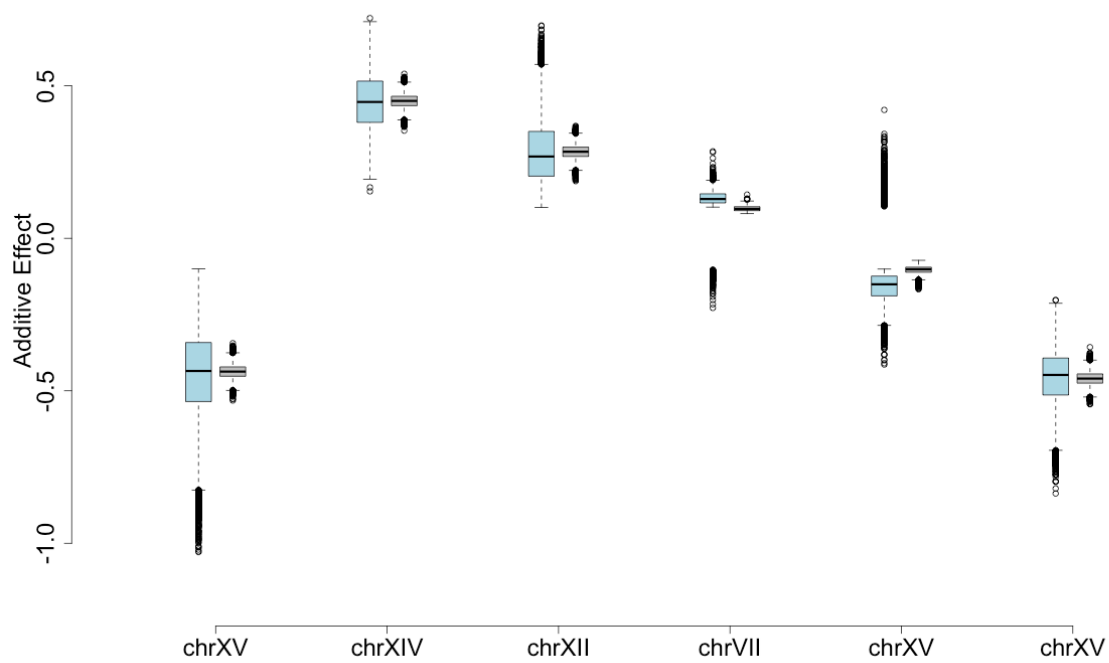


**Figure S53. Additive phenotypic effect across simulated populations, Lactate network 2.**

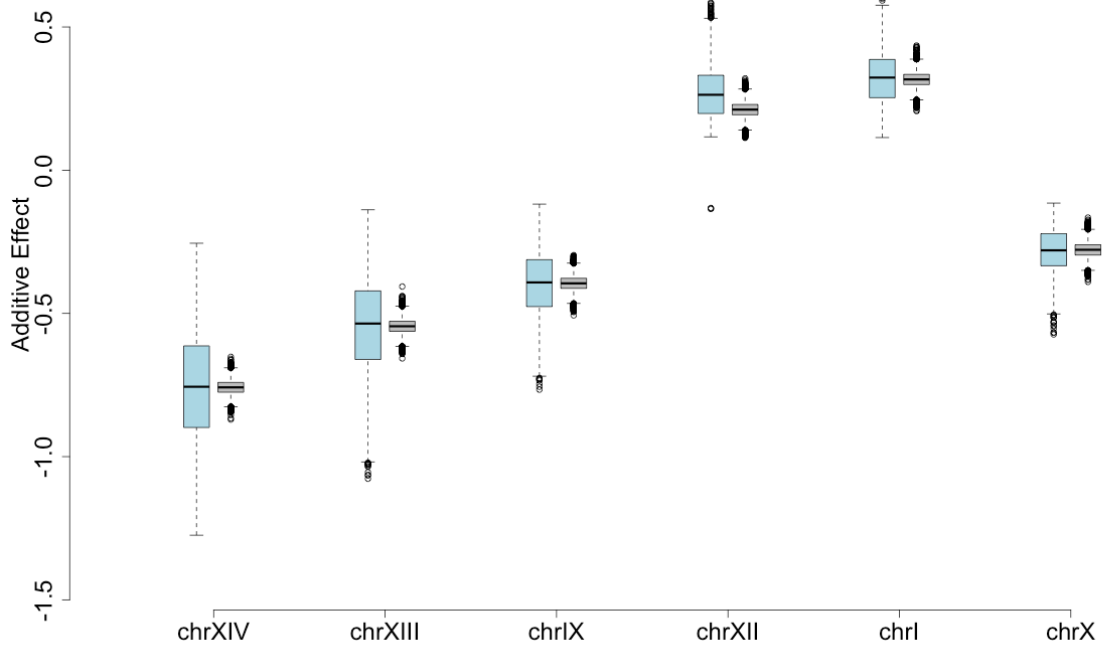


**Figure S54.** Additive phenotypic effect across simulated populations, *E6-Berberine*.

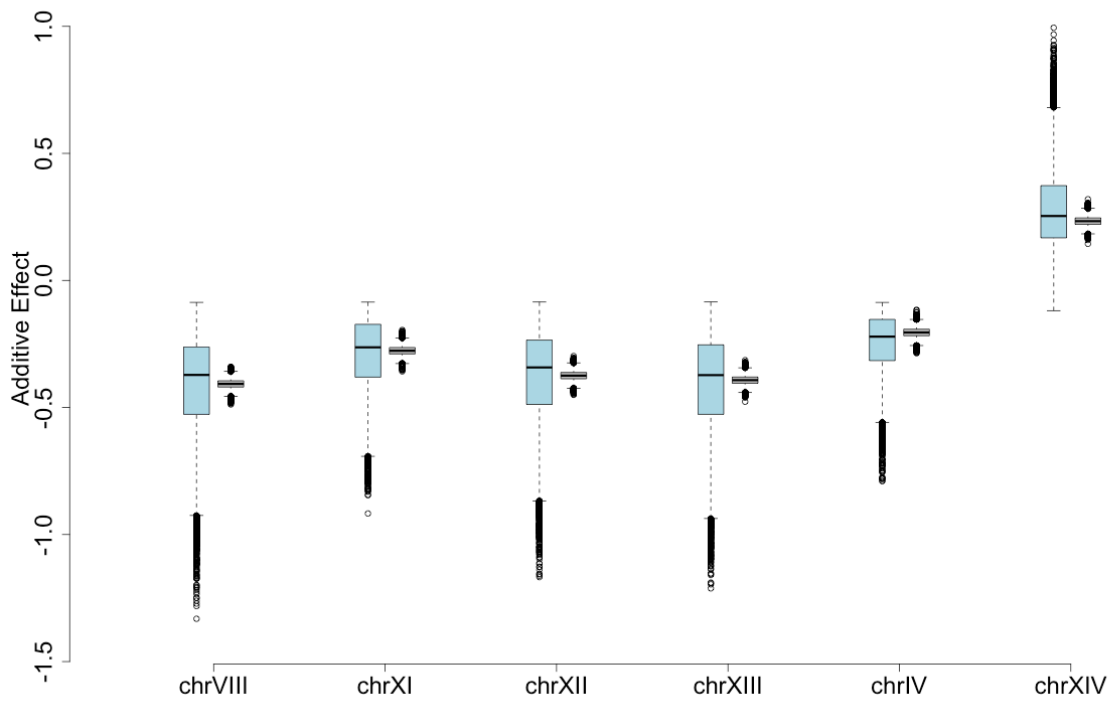


**Figure S55.** Additive phenotypic effect across simulated populations, *Copper Sulfate*.

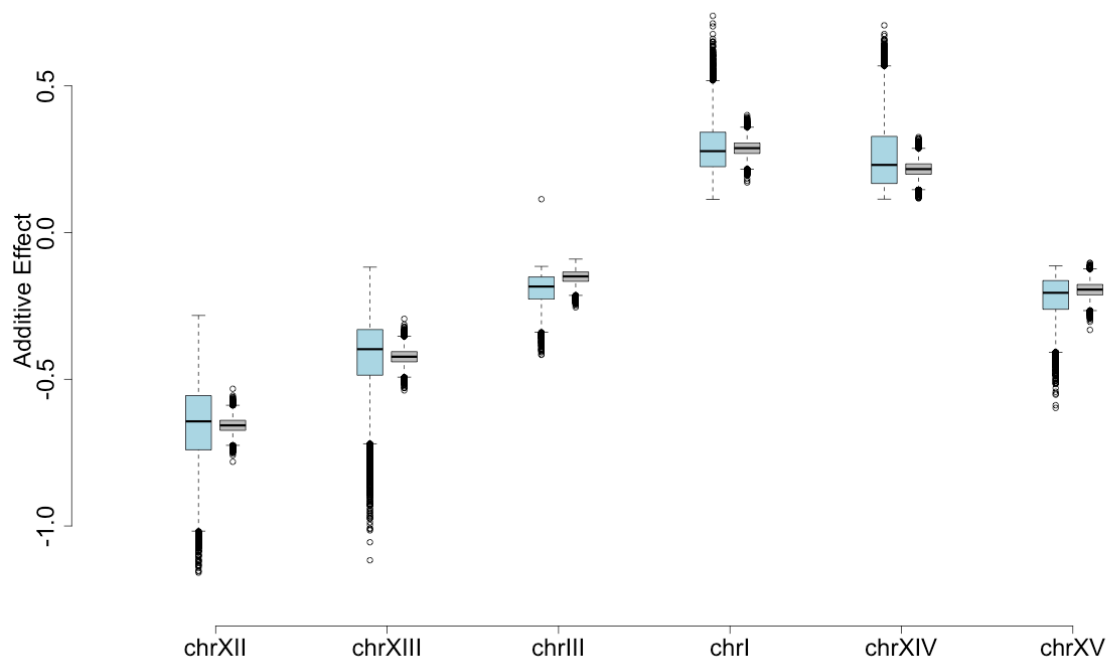


*Figure S56. Additive phenotypic effect across simulated populations, Cobalt Chloride.*